PB-229 102

# AERODYNAMIC CONTROL OF NITROGEN OXIDES AND OTHER POLLUTANTS FROM FOSSIL FUEL COMBUSTION

## VOLUME I. DATA ANALYSIS AND SUMMARY OF CONCLUSIONS

INSTITUTE OF GAS TECHNOLOGY

PREPARED FOR
ENVIRONMENTAL PROTECTION AGENCY

OCTOBER 1973

DISTRIBUTED BY:

NTIS
National Technical Information Service
U. S. DEPARTMENT OF COMMERCE

| BIBLIOGRAPHIC DATA SHEET | 1. Report No. EPA-650/2-73-033a | 2. | PB 229 102 |
|---|---|---|---|

4. Title and Subtitle
Aerodynamic Control of Nitrogen Oxides and Other Pollutants from Fossil Fuel Combustion
Volume I--Data Analysis and Summary of Conclusions

5. Report Date: October 1973

6.

7. Author(s): D. R. Shoffstall and D. H. Larson

8. Performing Organization Rept. No.

9. Performing Organization Name and Address
Institute of Gas Technology
IIT Center
3424 South State Street, Chicago, Illinois 60616

10. Project/Task/Work Unit No.

11. Contract/Grant No.: 68-02-0216

12. Sponsoring Organization Name and Address
EPA, Office of Research and Development
NERC-RTP, Control Systems Laboratory
Research Triangle Park, North Carolina 27711

13. Type of Report & Period Covered: Final

14.

15. Supplementary Notes

16. Abstracts
The report gives a synopsis of data collected from investigating the relationship between combustion, aerodynamics, and pollutant emission characteristics of industrial burners. Five types of burners were studied: a scaled-down utility power boiler burner; a high-intensity (flat-flame) burner; a movable-block burner developed by the International Flame Research Foundation; an axial flow burner; and a baffle burner used in steel reheat furnaces. Broad conclusions, applicable to all burners tested, were: burners using radial gas injection produce peak NO at 11% or less excess air; burners using axial gas injection produce peak NO at 22% or more excess air; NO concentration increases with increasing air preheat, but the magnitude of the change depends on burner design and the gas injection method; and changing from axial to radial gas injection consistently results in an increase in NO concentration. Volume II is subtitled Raw Data and Experimental Equipment.

17. Key Words and Document Analysis. 17a. Descriptors
Air Pollution
Nitrogen Oxides
Aerodynamics
Natural Gas
Combustion Control
Burners
Flames

17b. Identifiers/Open-Ended Terms
Air Pollution Control
Stationary Sources
Axial Injection
Radial Injection
Swirl
Type I Flame
Type II Flame
Radial Profiles
Industrial Burners

17c. COSATI Field/Group: 13B, 21B

| 18. Availability Statement | 19. Security Class (This Report) | 21. No. of Pages |
|---|---|---|
| Unlimited | UNCLASSIFIED | ~~80~~ 83 |
| | 20. Security Class (This Page) UNCLASSIFIED | 22. Price 4.00 / 1.45 |

PB-229-102

EPA-650/2-73-033a

# AERODYNAMIC CONTROL OF NITROGEN OXIDES AND OTHER POLLUTANTS FROM FOSSIL FUEL COMBUSTION

## VOLUME I. DATA ANALYSIS AND SUMMARY OF CONCLUSIONS

by

D.R. Shoffstall and D.H. Larson

Institute of Gas Technology
IIT Center, 3424 South State Street
Chicago, Illinois 60616

Contract No. 68-02-0216
Program Element No. 1A2014
ROAP No. 21ADG47

EPA Project Officer: David W. Pershing

Control Systems Laboratory
National Environmental Research Center
Research Triangle Park, North Carolina 27711

Prepared for

OFFICE OF RESEARCH AND DEVELOPMENT
U.S. ENVIRONMENTAL PROTECTION AGENCY
WASHINGTON, D.C. 20460

1-A

October 1973

This report has been reviewed by the Environmental Protection Agency and approved for publication. Approval does not signify that the contents necessarily reflect the views and policies of the Agency, nor does mention of trade names or commercial products constitute endorsement or recommendation for use.

TABLE OF CONTENTS


| | Page |
|---|---|
| INTRODUCTION | 1 |
| SUMMARY OF CONCLUSIONS | 2 |
| Input-Output Test Results | 2 |
| In-the-Flame Mapping | 2 |
| RESEARCH INSTALLATION | 3 |
| GENERAL CHARACTERIZATION OF THE FLAME | 4 |
| DATA ANALYSIS AND DISCUSSION | 8 |
| Baffle Burner | 8 |
| "Intermediate" Flame Baffle Burner | 8 |
| "Short" Flame Baffle Burner | 18 |
| Movable-Block Swirl Burner (I.F.R.F. Design) | 27 |
| Flat-Flame Burner | 38 |
| Boiler Burner | 46 |
| GENERAL OBSERVATIONS | 57 |

LIST OF FIGURES


| Figure No. | | Page |
|---|---|---|
| I-1 | Toroidal Recirculating Cell for a Typical Type I Flame | 6 |
| I-2 | Steady Pear-Shaped Recirculating Cell for a Typical Type II Flame | 7 |
| I-3 | Assembly Drawing of Axial-Flow Burner With Ported Swirl Baffles | 9 |
| I-4 | Modified Gas Nozzle Construction | 10 |
| I-5 | Normalized NO Concentration as a Function of Excess Air | 12 |
| I-6 | Radial Profile for NO at the 5-cm Axial Position | 13 |
| I-7 | Normalized NO Concentration as a Function of Excess Air | 15 |
| I-8 | Radial Profile for NO at the 5-cm Axial Position | 16 |
| I-9 | Temperature Profile Across Furnace With Gas Input of 2546 CF/hr and 5.0-cm Axial Probe Position | 17 |
| I-10 | Normalized NO Concentration as a Function of Excess Air | 19 |
| I-11 | Normalized NO Concentrations as a Function of Excess Air | 21 |
| I-12 | Radial Profile for NO at the 7.6-cm Axial Position | 22 |
| I-13 | Radial Temperature Profile at the 7.6-cm Axial Position | 23 |
| I-14 | Radial Profile for NO Concentration for the Short-Flame Baffle Burner Using the Axial Nozzle at a 7.6-cm Axial Position | 26 |
| I-15 | Diagram of a Movable-Block Swirl Burner | 28 |
| I-16 | Arrangement of Swirl Generating Blocks in the Movable-Block Swirl Burner | 29 |
| I-17 | Normalized NO Concentration as a Function of Excess Air | 31 |
| I-18 | Normalized NO Concentration as a Function of Excess Air | 32 |

LIST OF FIGURES, Cont.


| Figure No. | | Page |
|---|---|---|
| I-19 | Normalized NO Concentration as a Function of Excess Air | 33 |
| I-20 | Normalized NO Concentration Profiles as a Function of Swirl Intensity and Excess Air on the Movable-Block Swirl Burner With Gas Nozzle in the Exit Position | 34 |
| I-21 | Normalized NO Concentration Profiles as a Function of Swirl Intensity and Excess Air on the Movable-Block Swirl Burner With Gas Nozzle in the Throat Position | 35 |
| I-22 | Radial Profile of NO Concentration at the 12.7-cm Axial Position for the Movable-Block Swirl Burner With Intermediate Intensity | 36 |
| I-23 | Radial NO Concentration Profile for the Movalbe-Block Burner at an Axial Probe Position of 12.7 cm and Set for Intermediate Swirl Intensity, Gas Nozzle in Throat Position, and a Gas Input of 2008 CF/hr | 37 |
| I-24 | Radial Temperature Profile at the 12.7-cm Axial Position | 39 |
| I-25 | Cross-Sectional View of the Flat-Flame High-Intensity Burner | 41 |
| I-26 | Normalized NO Concentration as a Function of Excess Air for the Flat-Flame Burner | 43 |
| I-27 | Radial NO Concentration Profile for the Flat-Flame Burner at a 12.7-cm Axial Position | 44 |
| I-28 | Radial Temperature Profiles for the Flat-Flame Burner at Axial Positions of 12.7, 69, and 130 cm | 45 |
| I-29 | Guide-Vane Boiler Burner | 47 |
| I-30 | Method for Measuring Guide-Vane Angle for Boiler Burner | 48 |
| I-31 | Normalized NO Concentration as a Function of Excess Air (Boiler Burner With a 30-deg Angle Vane Setting; Gas Input, 3020 CF/hr) | 49 |

LIST OF FIGURES, Cont.


| Figure No. | | Page |
|---|---|---|
| I-32 | Normalized NO Concentration as a Function of Excess Air (Boiler Burner With a 40-deg Angle Vane Setting; Gas Input, 3040 CF/hr) | 50 |
| I-33 | Normalized NO Concentration as a Function of Excess Air (Boiler Burner With a 60-deg Angle Vane Setting; Gas Input, 3040 CF/hr) | 51 |
| I-34 | NO Concentration Versus Swirl Number | 53 |
| I-35 | Radial Profile for NO at a 60-deg Vane Angle Setting | 54 |
| I-36 | Radial Temperature Profile | 55 |
| I-37 | Radial NO Concentration Profile for the Movable-Block Burner at an Axial Probe Position of 12.7 cm and Set for Intermediate Swirl Intensity, Gas Nozzle in Throat Position, 3.6% Excess Oxygen, and a Gas Input of 2008 CF/hr | 58 |
| I-38 | Radial $CH_4$ Concentration Profile for the Movable-Block Burner at an Axial Probe Position of 12.7 cm and Set for Intermediate Swirl Intensity, Gas Nozzle in Throat Position, 3.6% Excess Oxygen, and a Gas Input of 2008 CF/hr | 59 |
| I-39 | Radial $O_2$ Concentration Profile for the Movable-Block Burner at an Axial Probe Position of 12.7 cm and Set for Intermediate Swirl Intensity, Gas Nozzle in Throat Position, 3.6% Excess Oxygen, and a Gas Input of 2008 CF/hr | 60 |
| I-40 | Radial Temperature Profile at the 12.7-cm Axial Position | 61 |
| I-41 | Radial Profile of Axial Velocity at the 12.7-cm Axial Position | 62 |
| I-42 | Infrared Spectra Band Locations | 63 |
| I-43 | NO Concentration Correction Factors for Gas Samples Containing $C_2H_4$ and/or $C_3H_6$ | 65 |
| I-44 | Unsteady Pear-Shaped Recirculating Cell | 69 |
| I-45 | Kidney-Shaped Recirculating Cell | 70 |

## LIST OF TABLES


| Table No. | | Page |
|---|---|---|
| I-1 | Flame Characteristics | 5 |
| I-2 | Mass Spectrometer Laboratory Analytical Report – Natural Gas Sample | 24 |
| I-3 | Mass Spectrometer Laboratory Analytical Report – Gas Sample for Short-Flame Baffle Burner Axial Gas Nozzle | 25 |
| I-4 | Mass Spectrometer Laboratory Analytical Report – Gas Sample for Movable-Block Swirl Burner | 40 |
| I-5 | Vane-Angle Setting Versus Swirl Number for Boiler Burner | 46 |
| I-6 | Mass Spectrometer Laboratory Analytical Report – Gas Sample for Boiler Burner | 56 |
| I-7 | Time-Averaged Directional Flow Data Obtained at the 12.7-cm Axial Position | 67 |
| I-8 | Time-Averaged Directional Flow Data at the 30.5-cm Axial Position and Obtained Using a Hubbard Probe | 68 |

# INTRODUCTION

This volume of the final report for EPA Contract No. 68-02-0216 presents a synopsis of data collected from investigating the relationship between combustion, aerodynamics, and pollution emission characteristics of industrial burners. Five types of industrial burners were studied. These were a) a utility power boiler burner, b) a high-intensity or flat-flame burner, c) a movable vane burner design developed by the International Flame Research Foundation, d) an axial flow burner, and e) a partial baffle burner of a design widely used in steel reheat furnaces. The utility boiler burner was scaled down to fit our experimental system. The aerodynamic characteristics of each burner were investigated in connection with their influence on the combustion process and on pollution emissions. The research was divided into two categories:

1. Input-output tests in which the nitric oxide (NO) concentration in the flue (as well as other flue gas components) was measured as a function of changes in combustion conditions, such as percent excess oxygen (air), preheat temperatures of the combustion air, and firing rate of natural gas.

2. Point-by-point in-the-flame tests were made to measure gas species concentrations, temperatures, and velocities (magnitude and direction), in an attempt to determine where and how the NO was being formed.

A companion publication (Volume II) presents all of the raw data and data plots collected during the program. Volume II also gives a detailed description of the experimental facility, including dimensional descriptions of the hot-modeling furnace, the cold-modeling furnace simulator, sampling probes, instrumentation, and the test burners.

## SUMMARY OF CONCLUSIONS

From our analysis of the data obtained in this study (Volumes I and II), we were able to reach the following broad conclusions. A comprehensive listing of the more specific conclusions reached for each burner tested is given at the beginning of the section discussing that burner.

### Input-Output Test Results

1. Type II* flames with radial gas injection as produced by the axial burner and the boiler burner with radial gas nozzle will have peak NO concentrations at an excess air level of 11% or less.

2. Type I* or Type II flames with axial gas injection, axial burner, swirl burner, or flat-flame burner with axial gas nozzle will produce their maximum NO emissions at an excess air level greater than 22%.

3. Although for all the burners tested the concentration of NO increases with increasing preheat temperature of the combustion air, the magnitude of the incremental change is dependent on the type of burner and the method of gas injection.

4. Changing from axial to radial gas injection consistently resulted in an increase in the NO concentration, which could be as large as 600 ppm.

### In-the-Flame Mapping

1. All NO radial profiles measured for flames with Type I flow patterns, typified by axial gas injection, resembled an upside down script "m" (ᔓᔓᔓ) in shape, while Type II flow patterns, typified by radial gas injection, resembled a "W" in shape.

2. For burners with a Type II flow pattern, more than 50% of the flue NO concentration is formed in the burner block.

3. Because only 50 to 80% of the flue NO concentration was measured in the flame for both Type I and Type II flow patterns, we postulate that secondary NO formation occurs either through a continuation of the nitrogen-oxygen type reactions or because of thermal decomposition of $NO_2$.

---

* A complete description of Type I and Type II flames is given in the section, "General Characterization of the Flame," beginning on page 4.

## RESEARCH INSTALLATION

All burners investigated were end-wall mounted on a 5 x 5 x 15 foot cast refractory furnace. The combustion air was heated ($100^0$ to $600^0$F) in an insulated electric preheater. Flue-gas samples were withdrawn through a water-cooled stainless-steel probe and approximately 50 feet of Teflon tubing into the various instrumentation remotely located from the furnace. Concentrations of CO, $CO_2$, $CH_4$, and NO were measured by multirange nondispersive infrared analyzers (NDIR). An electrolytic analyzer was used to measure oxygen. The output signals from the NDIR analyzers were time-averaged electrically and displayed on digital voltmeters. Flow direction and magnitude in the furnace were measured with both a five-hole pitot probe and a Hubbard probe. The pressure differentials between probe tip holes used for determining flow direction and velocity are measured with an electrical transducer. The signal from the transducer is analyzed and displayed on a multirange electronic manometer.

Temperatures are measured on a high-velocity suction pyrometer containing a Pt – Pt 13% Rd thermocouple which has been calibrated against flow rate through the tip. Output voltages from the thermocouple are read directly by a millivolt electrometer. Volume II of this report presents more detailed information on the installation.

## GENERAL CHARACTERIZATION OF THE FLAME

Table I-1 gives a synopsis of the work being reported. The first two columns of the table give the burner type and the kind of gas nozzle being investigated. The characteristic flame type of the burner-nozzle combination is listed in column 3. Columns 4 through 8 give the conditions at which the furnace was set during the in-flame studies, with the final two columns giving NO radial-profile data.

A general aerodynamic characterization of the burners can be made by detining types of flow patterns observed in the flame. A flame may be divided into four zones of interest: 1) the methane-rich central forward flow zone, 2) the combustion air forward flow zones, 3) the internal reverse flow zones, and 4) the secondary recirculation zones. For the Type I flame shown in Figure I-1, the methane-rich jet flows along the axis of the burner and has a velocity large enough to penetrate the internal reverse-flow regions, which are represented by the lobes on each side of the burner's axis. The combustion air circulates around the outside edge of each of the reversal lobes. The (— · — · —) lines in Figure I-1 represent the boundary layers between the forward flow of the combustion air and the secondary recirculation patterns of the combustion products. Characteristics of Type I flames found during our investigation are 1) a long, lazy, and luminous flame; 2) a high methane concentration, not only on the axis of the burner but also in the internal recirculation lobes; and 3) in general, the stoichiometric ratio of fuel and air accompanied by peak temperatures occurring on the outside edge of the internal recirculation lobes.

The Type II flame is characterized by inability of the central methane jet to penetrate the internal recirculation zone, as is shown in Figure II-2. This flame type can be generated either by introducing the gas radially with respect to the axis of the burner or by having an air flow with such a large tangential-velocity component that it attaches to the wall of the burner block and encloses a large toroidal vortex reverse flow zone situated on the axis of the burner. This pattern enables a matching of highly turbulent intensity zones with zones of high fuel concentration, resulting in a large combustion intensity. Characteristics of the Type II flame are 1) a short, translucent flame and 2) approximately 95% of the combustion's occurring in the burner block.

## Table I-1. FLAME CHARACTERISTICS

| Burner Type | Gas Nozzle | Flame Characterization: Flame Type | Gas Input, CF/hr | Wall Temp, °F | NO in Flue (Normalized), ppm | $O_2$ in Flue, % | Preheat Temp, °F | NO Profile: Position, cm | NO Profile: Concentration, ppm |
|---|---|---|---|---|---|---|---|---|---|
| Axial, Intermediate Baffle | Axial | I | 2147 | 2570 | 255 (286) | 2.6 | 570 | 0 | (160) |
| | | | | | | | | 18 | 54 |
| | | | | | | | | 30 | 142 |
| | Radial | II | 2547 | 2680 | 741 (800) | 1.7 | 510 | 0 | 502 |
| | | | | | | | | 16 | 344 |
| | | | | | | | | 45 | 666 |
| Axial, Short Baffle | Axial | I | 2190 | 2570 | 189 (215) | 2.9 | 315 | 0 | 142 |
| | | | | | | | | 21 | 69 |
| | | | | | | | | 54 | 174 |
| | Axial | I | 2190 | 2524 | 325 (369) | 3.0 | 515 | 0 | 202 |
| | | | | | | | | 21 | 121 |
| | | | | | | | | 54 | 276 |
| Swirl, Movable Block | Axial (Intermediate Swirl Intensity) | I | 2008 | 2453 | 111 (130) | 3.6 | -- | 0 | 5 |
| | | | | | | | | 12 | 13 |
| | | | | | | | | 45 | 40 |
| Flat Flame | Axial | II | 2010 | 2480 | 89 (109) | 4.4 | -- | 0 | 79 |
| | | | | | | | | 24 | 89 |
| | | | | | | | | 54 | 92 |
| Boiler | Radial | II | 3049 | 2534 | 283 (308) | 1.9 | 270 | 0 | 242 |
| | | | | | | | | 27 | 136 |
| | | | | | | | | 34 | 265 |

B-83-1308

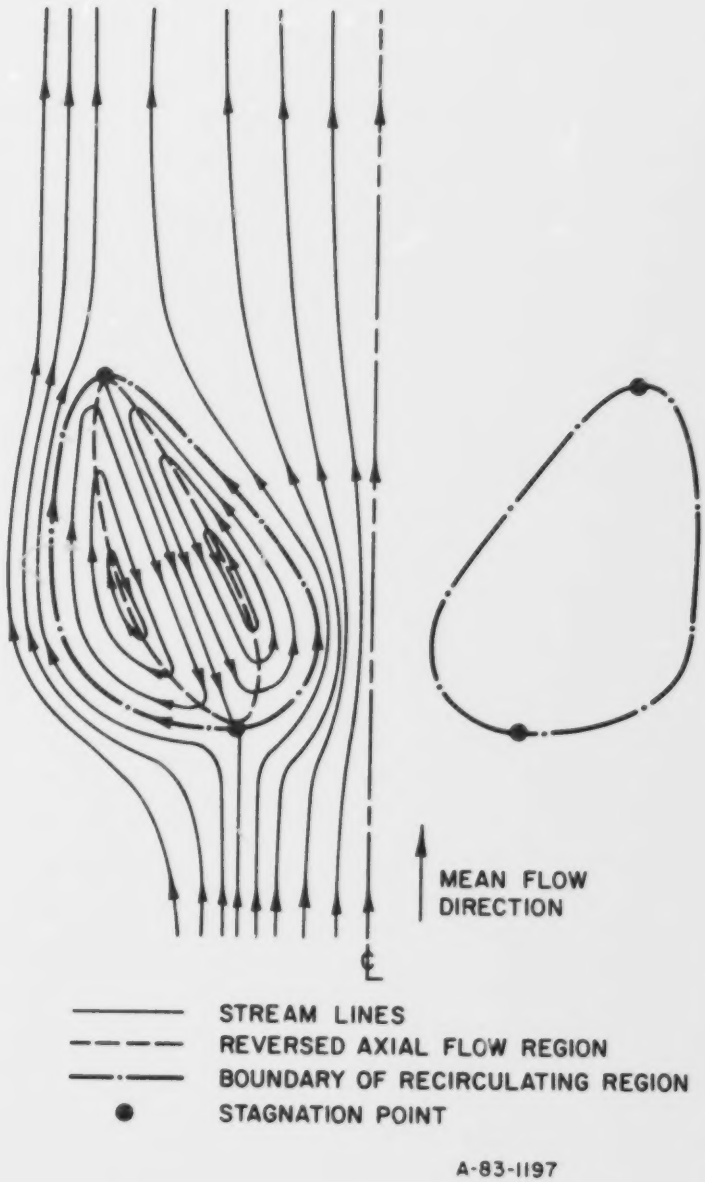


Figure I-1. TOROIDAL RECIRCULATING CELL FOR A TYPICAL TYPE I FLAME

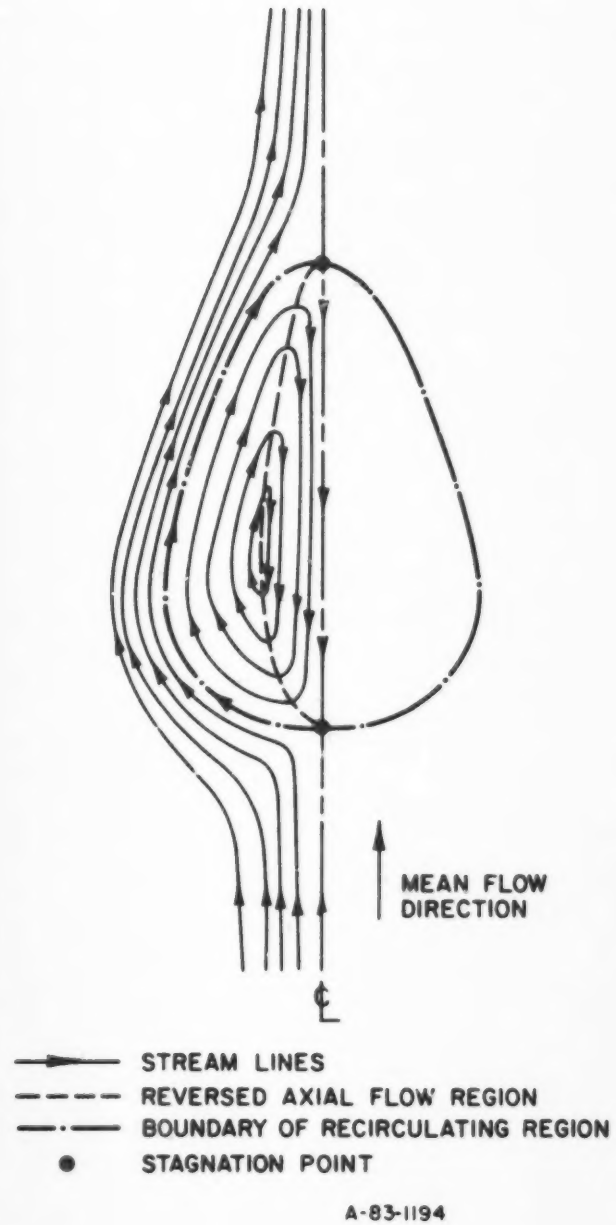


Figure I-2. STEADY PEAR-SHAPED RECIRCULATING CELL FOR A TYPICAL TYPE II FLAME

## DATA ANALYSIS AND DISCUSSION

### Baffle Burner

Figure I-3 illustrates the design of the baffle burner. The gas nozzle lies parallel to and along the axis of the burner. It is inserted into the ceramic baffle, thus ensuring that the gas will enter parallel to the axis of the baffle burner. Combustion air enters perpendicular to the axis and passes through the six ports in the baffle, which impart a swirl to the air in some designs. Two of these baffle ports can be seen in Figure I-3 with their axes parallel to the axis of the burner. Air exiting from the ports as illustrated would have an axial velocity component only, resulting in a "long" flame. To shorten the flame length, a radial- and tangential-flow component must be added to the combustion air velocity. This is accomplished by using a baffle where the combustion-air ports are rotated relative to the axis of the burner. For the "intermediate" flame length baffle the rotation orientation of the ports is 12 degrees and for the "short" flame length, 24 degrees. Figure I-4 shows the gas nozzle modifications needed to achieve radial gas injection for the baffle burner. Basically the nozzle end is capped and a series of holes are drilled radially in the tube wall.

### "Intermediate" Flame Baffle Burner

Based on an analysis of the input-output data for the intermediate-flame baffle, we determined the following:

1. As expected, both increased gas input and increased preheat temperature significantly increased NO emissions. The change in NO emissions was more strongly affected by changes in preheat temperature. On the average, NO emissions increased 300% for a 600°F preheated air temperature increase and 25% for a 800 CF/hr increase in gas input.

2. The emissions of NO as a function of the percent of excess air (oxygen) showed the characteristic "bell-shaped" relationship. For the radial gas nozzle, the NO emissions peaked at about 2% oxygen (10% excess air). This peak shifted to higher excess-air levels when the gas-air mixing rate was decreased (longer flames).

3. We found that the slow mixing gases of a long flame generally produce one-third as much NO as the fast-mixed gases of a very short flame. When the burner nozzle was modified so that the combustion mixing was slowed down, the flame length increased from about 2 feet to over 13 feet, and the NO concentration decreased from an average of 700 ppm to 200 ppm.

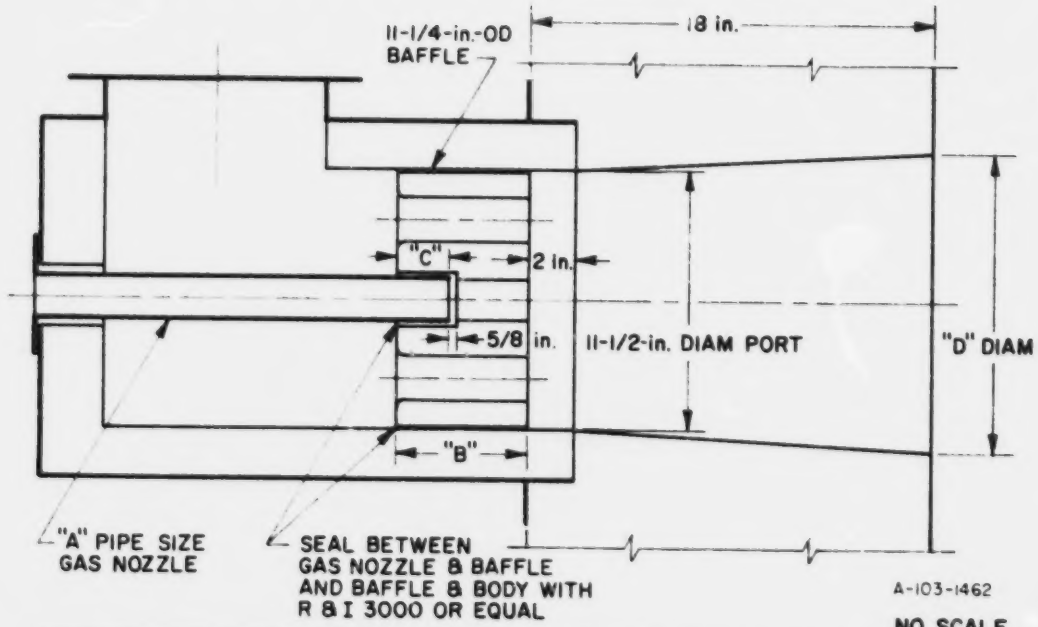


| BAFFLE | AIR PRESSURE FOR 40,000 SCF/hr at 850 °F | "A" | "B" | "C" | "D" |
|---|---|---|---|---|---|
| a. LONG FLAME | 3.25 in. wc | 1-1/4 in. | 6 in. | 2-3/8 in. | 13 in. |
| b. SHORT FLAME | 18 in. wc | 3/4 in. | 5 in. | 2-3/8 in. | 16-1/2 in. |
| c. INTER. FLAME | 14 in. wc | 1 in. | 8 in. | 3-7/8 in. | 13 in. |

Figure I-3. ASSEMBLY DRAWING OF AXIAL-FLOW BURNER WITH PORTED SWIRL BAFFLES

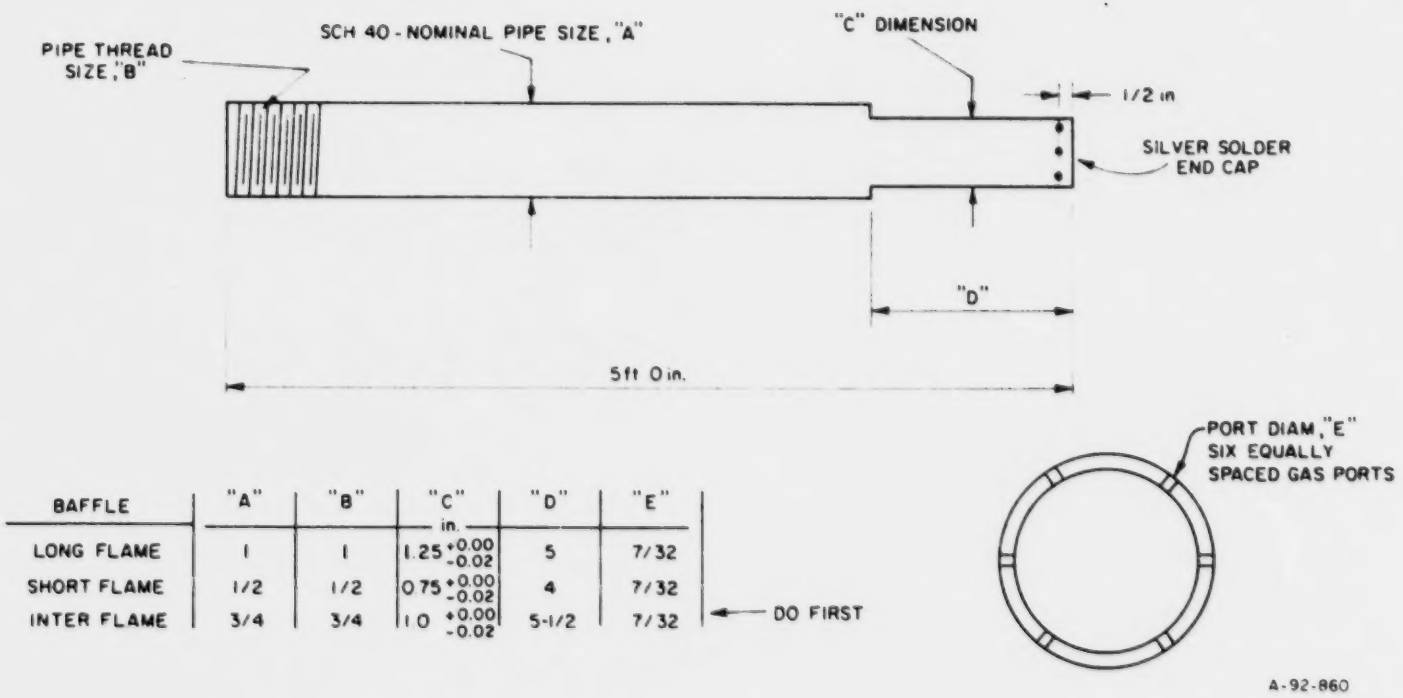


| BAFFLE | "A" | "B" | "C" in. | "D" | "E" | |
|---|---|---|---|---|---|---|
| LONG FLAME | 1 | 1 | $1.25^{+0.00}_{-0.02}$ | 5 | 7/32 | |
| SHORT FLAME | 1/2 | 1/2 | $0.75^{+0.00}_{-0.02}$ | 4 | 7/32 | |
| INTER FLAME | 3/4 | 3/4 | $1.0^{+0.00}_{-0.02}$ | 5-1/2 | 7/32 | ← DO FIRST |

Figure I-4. MODIFIED GAS NOZZLE CONSTRUCTION

4. We also found that the change in NO emissions as a result of changing gas input is larger at higher preheat temperatures. Increasing the gas input from 2300 CF/hr to 3100 CF/hr at a 100°F preheat temperature generally resulted in a 75-ppm increase in NO. However, increasing the gas the same amount while using 450°F preheated air resulted in an average NO emission increase of 150 ppm.

The flame from the axial burner with the intermediate baffle and the axial gas nozzle exhibited a Type I directional flow pattern. The burner block had a 2.7-degree divergent angle with a 16.5-cm radius at the inside edge of the furnace wall.

Typical measured NO concentrations in the flue as a function of percent excess oxygen (air) using the axial burner, intermediate-flame baffle, and axial gas nozzle are shown in Figure I-5. These data were gathered at a 2147 CF/hr gas input for combustion air preheat temperatures of 100°, 270°, and 570°F. The NO concentrations presented in this paper as input-output test results were normalized by dividing the weight of the flue products at the stoichiometric mixture of fuel and air into the measured concentration of NO, and multiplying this ratio by the weight of the flue products for the input conditions under which the measurements were taken.

Each curve in Figure I-5 displays a different positive slope for the change in normalized NO concentration vs. percent of excess oxygen. Note that no point of inflection is shown by these curves. Measured concentrations of carbon monoxide greater than 100 ppm are denoted by listing their numerical value in parts per million next to the appropriate data point.

Figure I-6 represents the radial profile for NO concentration in the flame and the secondary recirculation zone at an axial position of 5 cm from the front wall of the furnace. The data were collected at a gas input of 2147 CF/hr with 2.6% excess oxygen in the flue and a 570°F preheat temperature of the combustion air. The NO concentration has a maximum value of 162 ppm on the axis of the burner. The concentration decreases to a minimum of 56 ppm at an 18-cm radial position and then increases in value to 144 ppm in the secondary recirculation zone. Assuming a symmetrical NO concentration profile close to the axis of the burner, a shape of the profile would resemble a "W." The central

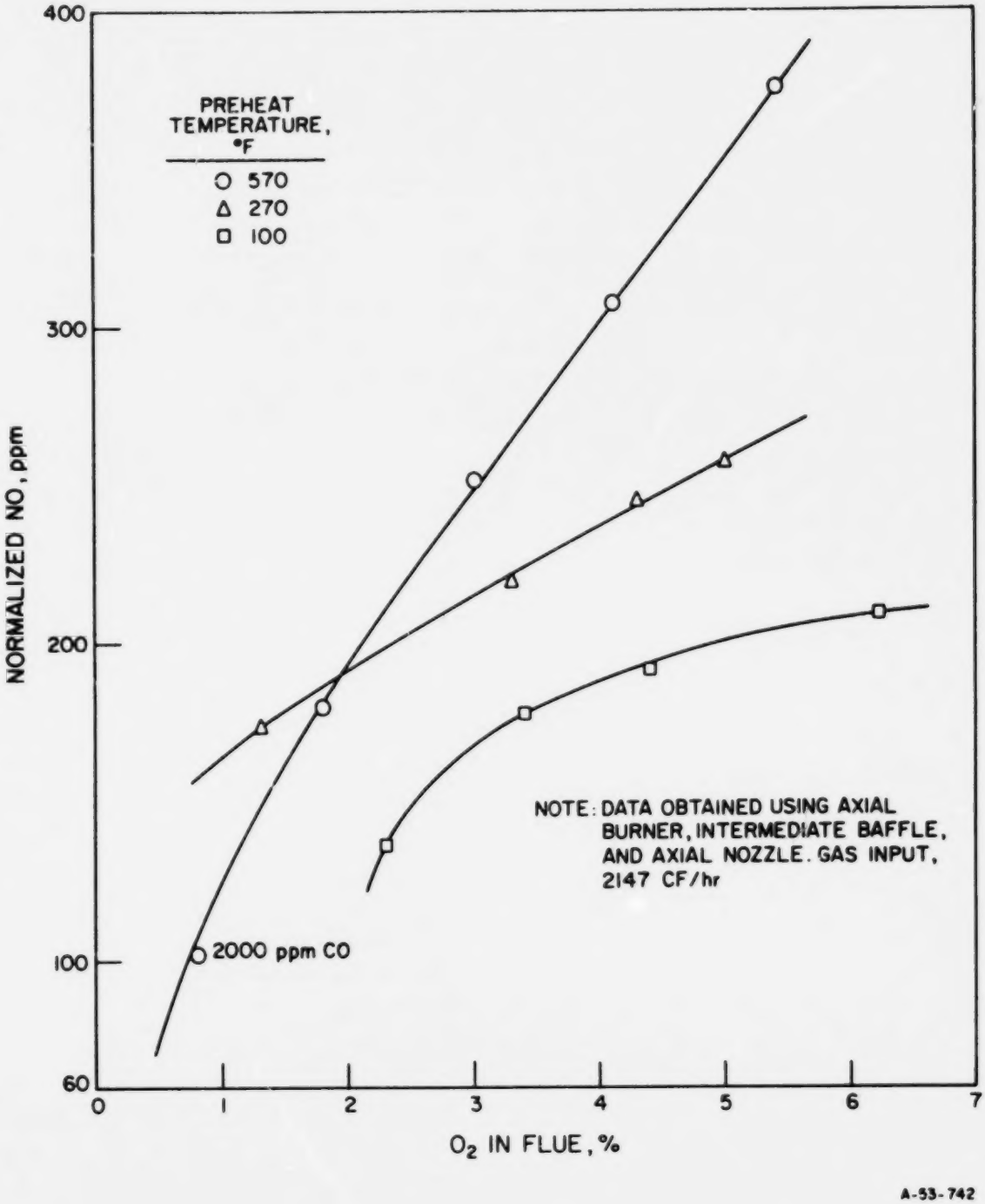


Figure I-5. NORMALIZED NO CONCENTRATION AS A FUNCTION OF EXCESS AIR

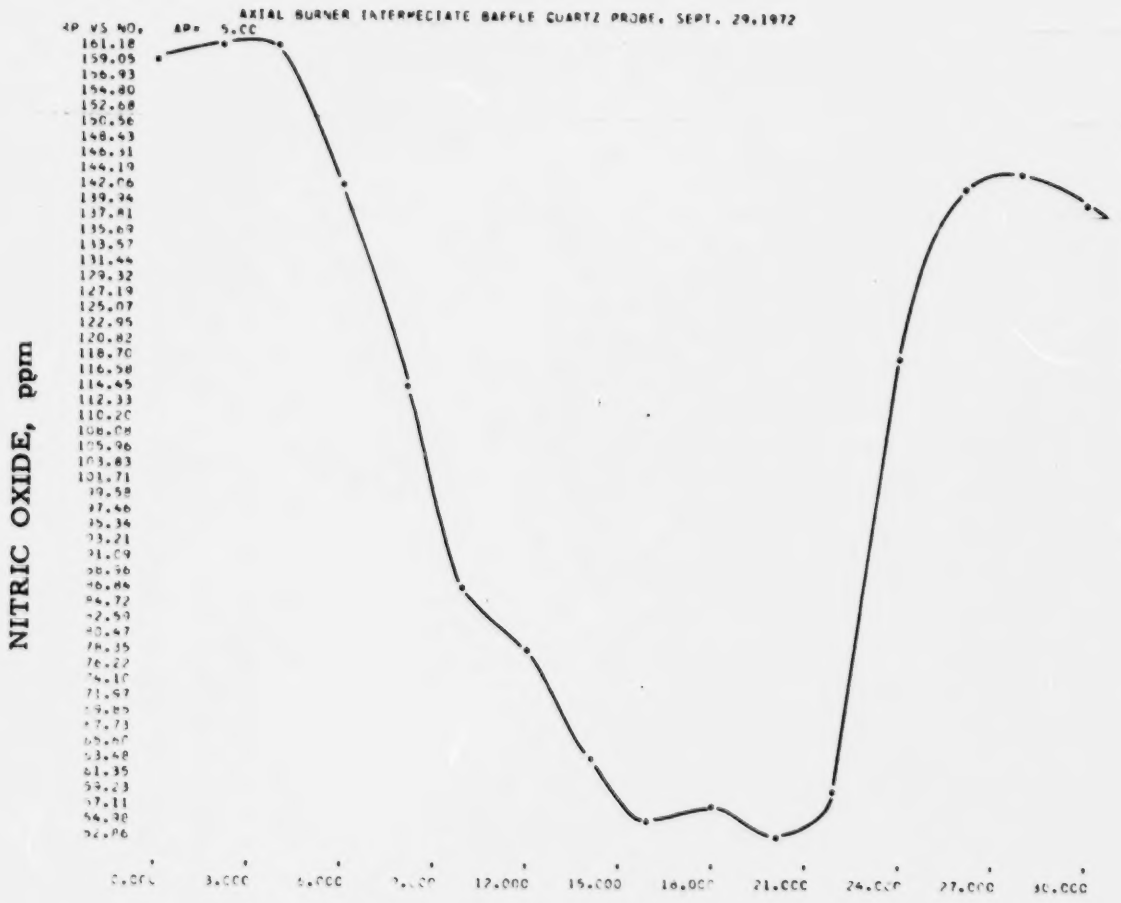


Figure I-6. RADIAL PROFILE FOR NO AT THE 5-cm AXIAL POSITION (Intermediate-Flame Baffle – Axial Gas Nozzle – Gas Input, 2147 CF/hr – Preheat Temperature, 570°F – 10% Excess Air)

point of inflection of the "W" shape would be on the axis of the burner and would contain a higher concentration of NO than the two end points of the "W" corresponding to NO concentrations in the secondary recirculation zone.

Figure I-7 gives the normalized NO concentrations as a function of percent excess oxygen in the flue for the "intermediate" flame baffle burner with the radial gas nozzle at a gas input of 2335 CF/hr and combustion air preheat temperatures of 100°, 295°, and 570°F. Because of the improved mixing conditions with radial gas injection, the minimum amount of excess air needed for proper combustion (defined as a flue concentration of carbon monoxide below 100 ppm) decreased by approximately 5% from the amount needed with axial gas injection. Each curve in Figure I-7 shows that the point of maximum NO concentration shifts toward higher percentages of excess oxygen as the air preheat temperature is increased. In addition, the values of the measured NO concentrations have increased by as much as 650 ppm from the levels measured with axial gas injection.

A NO concentration profile for the axial burner with an intermediate-flame baffle and radial gas nozzle is plotted in Figure I-8. These data were derived at a higher gas input of 2547 CF/hr with 10% excess air at a 510°F preheat air temperature. On the axis of the burner the measured NO concentration was 502 ppm. The concentration value decreases to a minimum of 346 ppm at a 16-cm radial position and then increases to a rather constant value of 655 ppm in the secondary recirculation zone. A symmetrical distribution of the NO profile about the axis of the burner again displays a "W"-shaped curve. However, unlike the profile produced by axial gas injection (Figure I-6), the maximum NO concentrations occurred in the secondary recirculation zones (at the ends of the W) rather than on the axis of the burner (corresponding to the central peak of the W).

A radial temperature profile for the furnace conditions listed in Table I-1 is shown in Figure I-9. The temperature is relatively constant in front of the burner block at about 3080°F. At a 28-cm radial position, the temperature begins to decrease rapidly until the secondary recirculation zone temperature of 2600°F is reached at a radial position

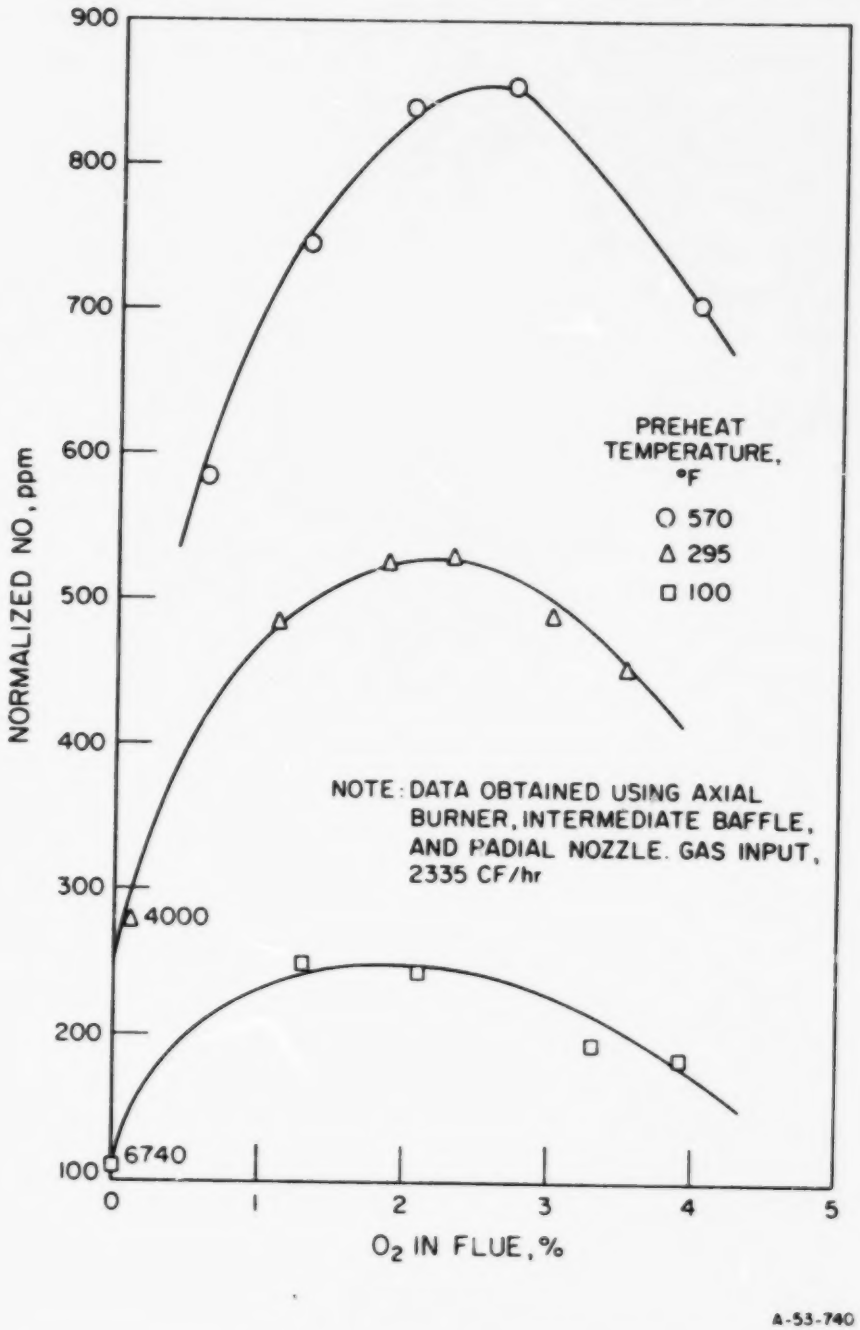


Figure I-7. NORMALIZED NO CONCENTRATION AS A FUNCTION OF EXCESS AIR

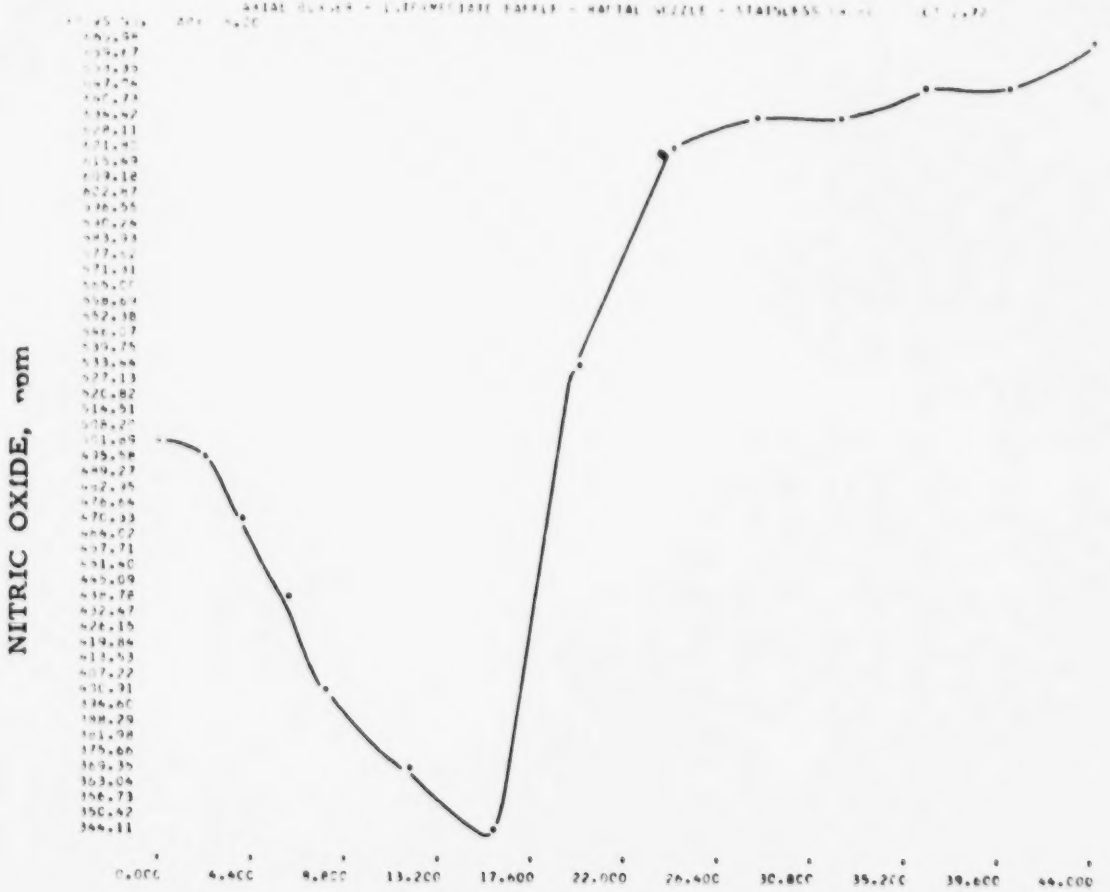


Figure I-8. RADIAL PROFILE FOR NO AT THE 5-cm AXIAL POSITION (Intermediate Flame Baffle – Radial Gas Nozzle – Gas Input, 2547 CF/hr – Preheat Temperatures, 510°F – 10% Excess Air)

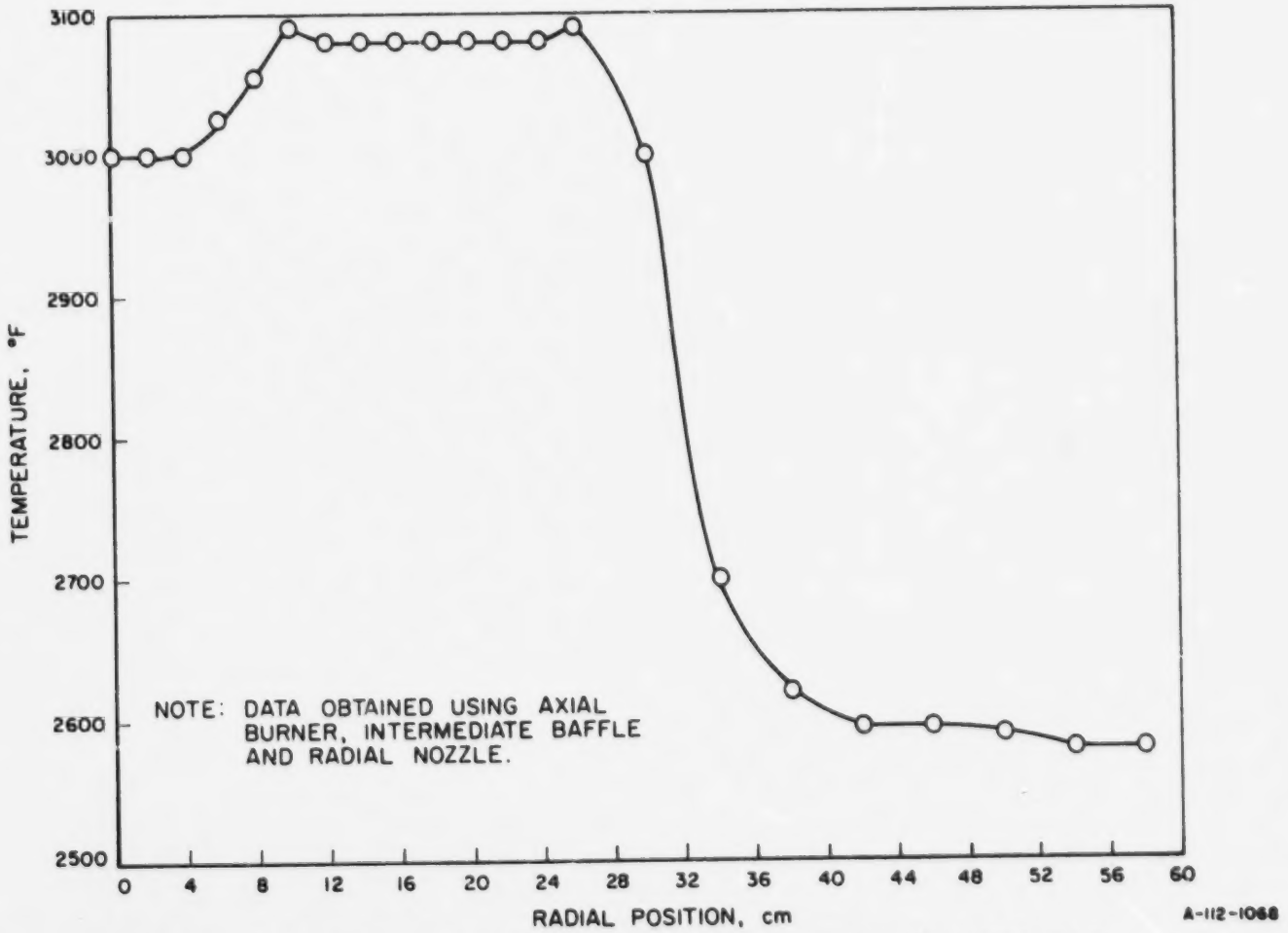


Figure I-9. TEMPERATURE PROFILE ACROSS FURNACE WITH GAS INPUT OF 2546 CF/hr AND 5.0-cm AXIAL PROBE POSITION

of 40 cm. The slight decrease in temperature between the axis of the burner and the 12-cm radial position may be caused by the central internal recirculation zone.

"Short" Flame Baffle Burner

Based on an analysis of the input-output data for the short-flame baffle, we determined the following:

1. As expected, both increased gas input and increased preheat temperature significantly increased NO emissions. The change in NO emissions was more strongly affected by changes in preheat temperature. On the average, NO emissions increased 200% for a 550°F preheat air temperature increase and 20% for a 500 CF/hr increase in gas input.

2. For the radial gas nozzle, the emissions of NO as a function of the percent of excess air (oxygen) showed the characteristic "bell-shaped" relationship. The NO emission peaked at about 2% oxygen (10% excess air). This peak shifted to higher excess air levels when the preheat air temperature was increased.

3. We found that the slow mixing gases of a long flame generally produce one-half as much NO as the fast mixing gases of a short flame. When the burner nozzle was modified so that the combustion mixing was slowed down, the flame length was visually observed to increase and the NO decreased from an average of 730 to 400 ppm.

Typical normalized NO concentrations in the flue as a function of percent excess oxygen and combustion air preheat temperature for the "short" flame baffle burner with a radial gas nozzle are shown in Figure I-10. This is a Type II flame. The gas input during these measurements was 2593 CF/hr. In comparison with the flue analysis data for the "intermediate" flame baffle burner (Figure I-7), there is an increase in the measured NO concentrations from the "short" flame baffle burner for the 100° and 300°F air preheat temperatures. Characteristically, the maximum NO concentrations occur at higher percentages of excess air as the preheat temperature of the air is increased.

The flame from the axial burner with the short baffle and an axial gas nozzle exhibited a Type I directional flow pattern. The burner block had an 8.9-degree divergent angle with a 21-cm radius at the hot face.

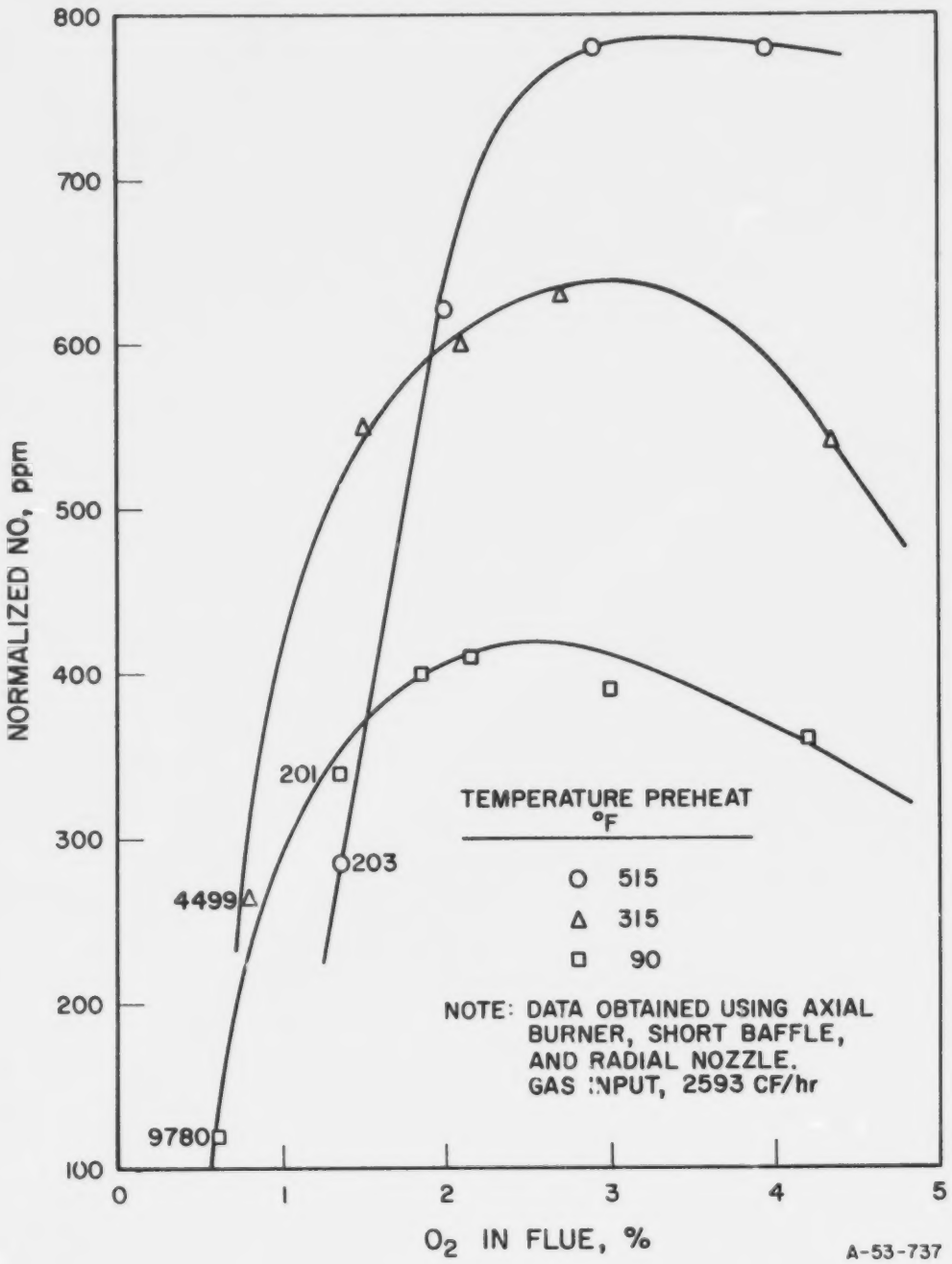


Figure I-10. NORMALIZED NO CONCENTRATION AS A FUNCTION OF EXCESS AIR

Figure I-11 illustrates normalized NO concentrations for a 2109 CF/hr gas input as a function of excess air and preheat temperature for the "short" flame baffle burner with axial gas injection. These graphs show greater curvature and higher concentrations of NO than those obtained from the intermediate baffle and axial gas nozzle (Figure I-5). As was the case for the intermediate baffle, the short-flame baffle with axial gas injection consistently produced lower NO concentrations than with radial gas injection for comparable levels of excess air.

A radial profile of the NO concentration at a 7.6-cm axial position with 15% excess air at a 315°F preheat temperature and a 2190 CF/hr gas input injected axially is illustrated in Figure I-12. The maximum "measured" NO concentration occurs along the axis of the burner with a 215 ppm peak concentration. At the 21-cm radial position a minimum value of 70 ppm is reached; the concentration then increases until it reaches a rather constant value of 172 ppm in the secondary recirculation zone. This profile resembles a "W" with the central inflection point higher than the two end points.

Figure I-13 shows the radial temperature profile for the same set of furnace conditions used when measuring the NO profile in Figure I-12. It should be noted that a "cold" temperature of 2070°F occurs at the 3-cm radial position, which corresponds to the location of the maximum "measured" NO concentration. The "hot" spots (2680°F and 2870°F) occur at +15 and −15 cm. (The stoichiometric ratio between oxygen and methane occurs between the radial positions of 15 and 18 cm and the radial positions of −12 and −15 cm.) The time-averaged NO concentrations at these points are 142 and 129 ppm, respectively. The central "cold" spot corresponds to the maximum methane concentration, whereas the "cold" spots at −18 and +21 cm are areas of relatively high oxygen concentrations (8.3% and 10.6%).

To investigate the possible formation of hydrocarbons in the flame, a grab sample was taken at the 0-cm radial position and at a 7.6-cm axial position. This sample was analyzed using a mass spectrometer; the results are listed in Table I-2. The natural gas used to fire the furnace was also analyzed and is shown in Table I-3. A comparison of these tables reveals that 0.4 mol % of ethylene ($C_2H_4$) and 0.5 mol % of acetylene ($C_2H_2$) were formed in the flame.

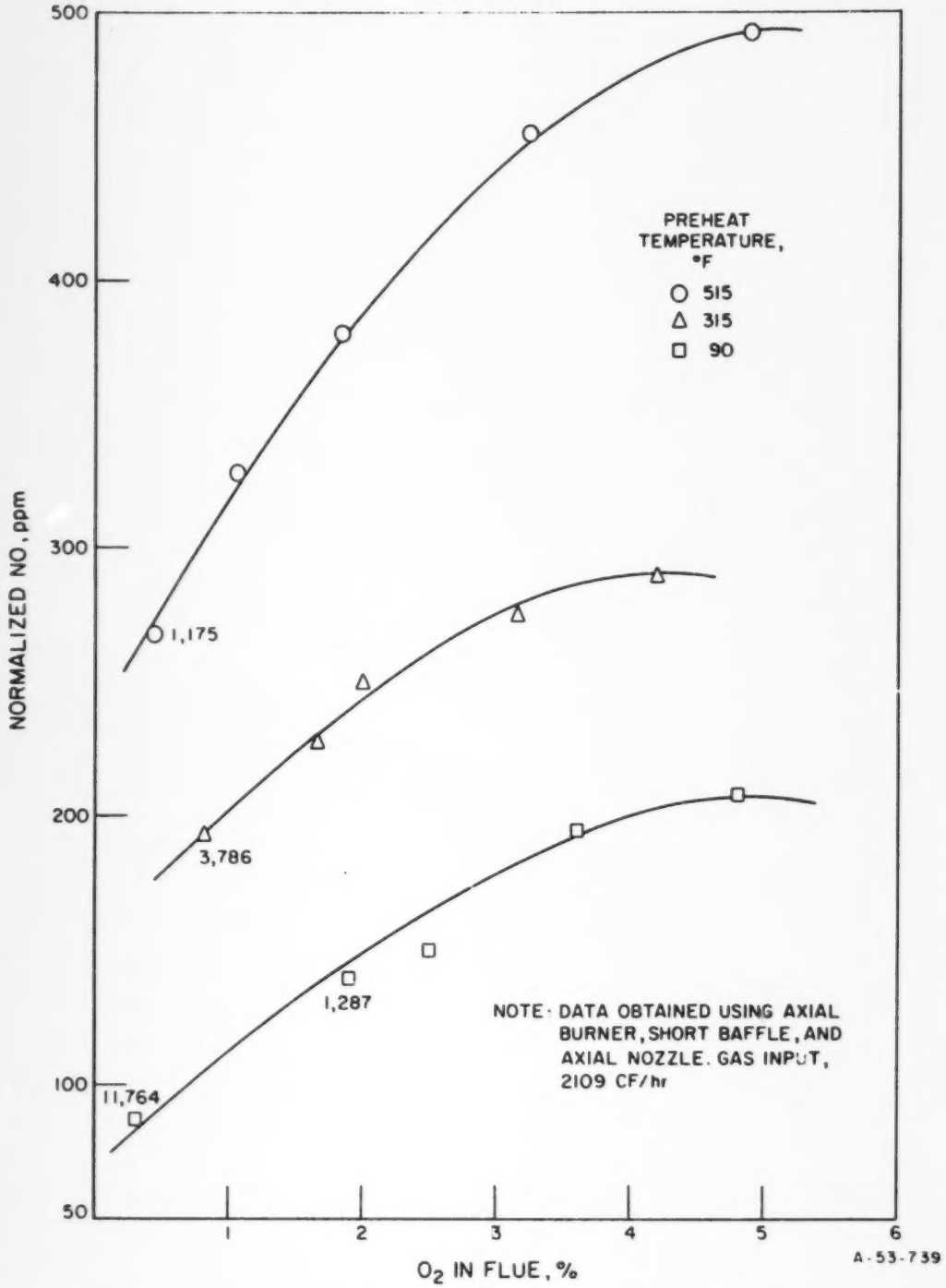


Figure I-11. NORMALIZED NO CONCENTRATION AS A FUNCTION OF EXCESS AIR

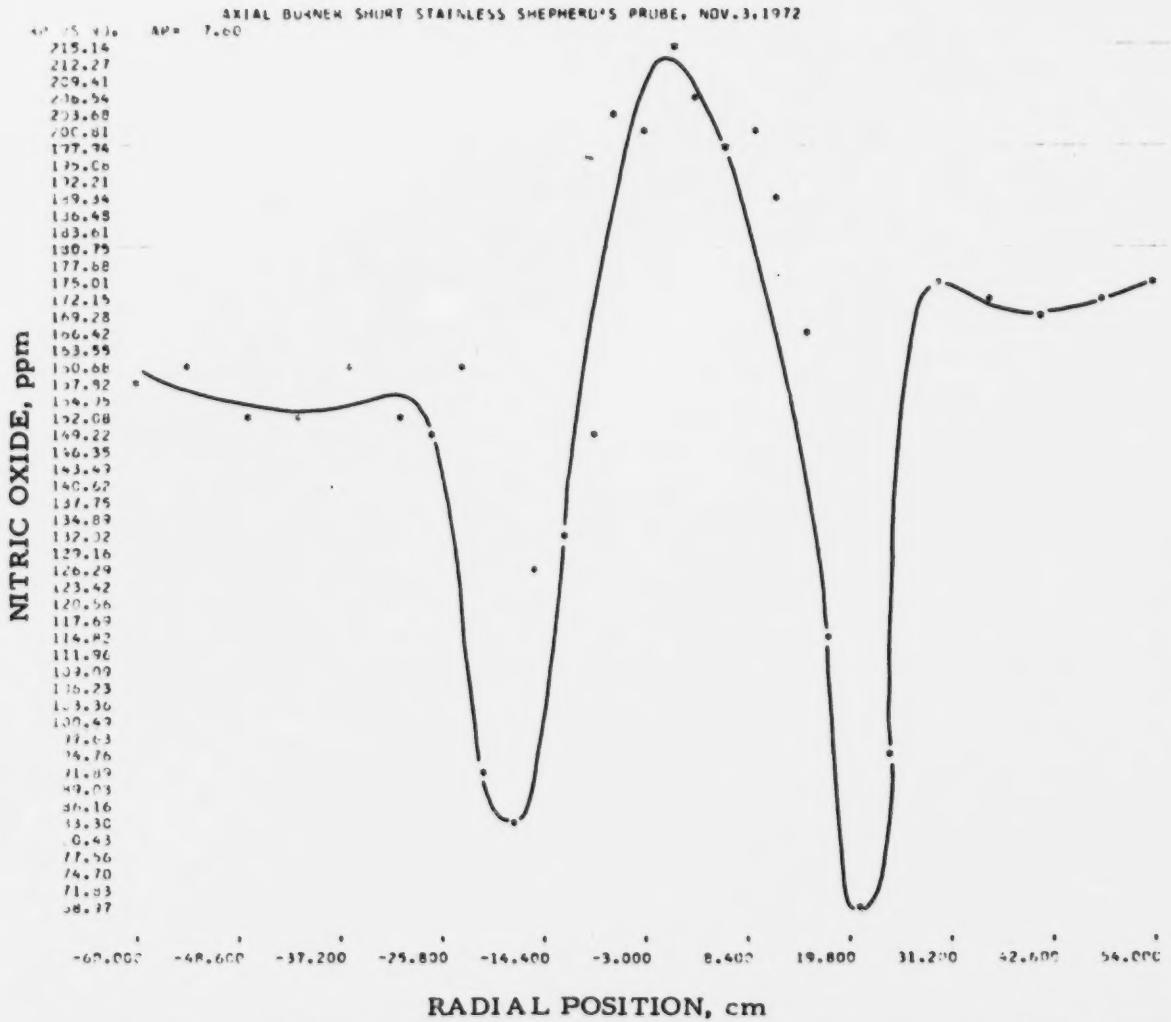


**Figure I-12. RADIAL PROFILE FOR NO AT THE 7.6-cm AXIAL POSITION (Short Flame Baffle – Axial Gas Nozzle – Gas Input, 2190 CF/hr – Preheat Temperature, 315°F – 3% Excess Air)**

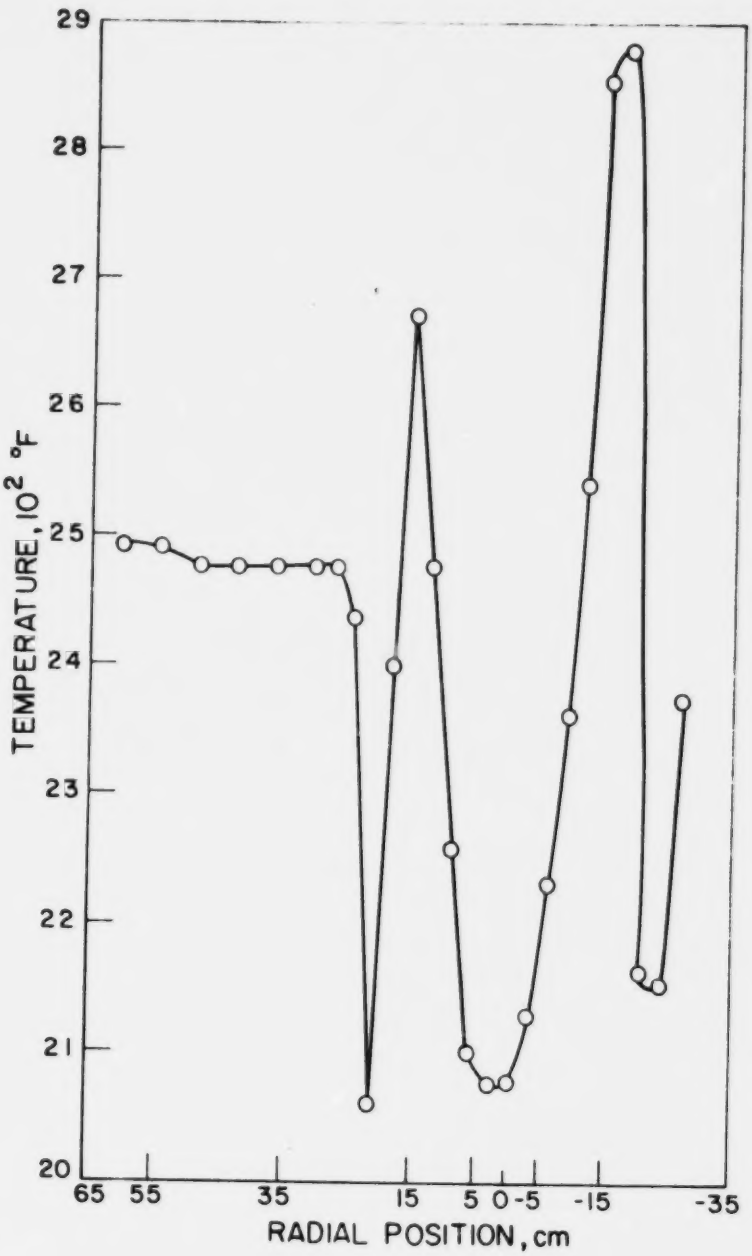


Figure I-13. RADIAL TEMPERATURE PROFILE AT THE 7.6 cm AXIAL POSITION (Short Flame Baffle – Axial Gas Nozzle – Gas Input, 2190 CF/hr – Preheat Temperature, 310°F – 3.3% Excess Oxygen)

Table I-2

**MASS SPECTROMETER LABORATORY**
**ANALYTICAL REPORT**

Material 8933 Sample # 2 11/16/72 Date 11/17/72

Requested by _____ M. S. Run No. 3289

| | Mol % | | Mol % |
|---|---|---|---|
| Nitrogen | 42.6 | Ethylene | 0.4 |
| Carbon Monoxide | 4.0 | Propylene | |
| Nitrogen+CO | | Butenes | |
| Oxygen | 2.4 | Pentenes | |
| Carbon Dioxide | 2.7 | Hexenes | |
| Hydrogen | 5.8 | | |
| Argon | 0.5 | 1,3-Butadiene | |
| Water Vapor | | Pentadienes | |
| Helium | | Cyclopentadiene | |
| Methane | 39.6 | Acetylene | 0.5 |
| Ethane | 1.2 | Diacetylene | |
| Propane | 0.0 | Methyl Acetylene | |
| n-Butane | 0.1 | +Propadiene | |
| Isobutane | | Vinyl Acetylene | |
| Pentanes | | Benzene | |
| Hexanes | | Toluene | |
| Heptanes | | Xylenes | |
| Octanes | | Ethyl Benzene | |
| | | Styrene | |
| | | Indene | |
| | | Napthalene | |
| | | TOTAL | 100.0 |

Calc. H. V., Btu SCF _____ Air Content _____

Calc. sp gr (Air 1.000) _____ Approved by _____

Table I-3

**MASS SPECTROMETER LABORATORY**
**ANALYTICAL REPORT**

Material 8933 Natural Gas from Pilot Plant  Date 11/8/72

Requested by _____  M. S. Run No. 3238

| | Mol % | | Mol % |
|---|---|---|---|
| Nitrogen | 2.40 | Ethylene | |
| Carbon Monoxide | | Propylene | |
| Nitrogen+CO | | Butenes | |
| Oxygen | | Pentenes | |
| Carbon Dioxide | 0.56 | Hexenes | |
| Hydrogen | | | |
| Argon | | 1,3-Butadiene | |
| Water Vapor | | Pentadienes | |
| Helium | 0.08 | Cyclopentadiene | |
| Methane | 91.74 | Acetylene | |
| Ethane | 3.93 | Diacetylene | |
| Propane | 0.95 | Methyl Acetylene | |
| n-Butane | 0.16 | +Propadiene | |
| Isobutane | 0.07 | Vinyl Acetylene | |
| Pentanes | 0.06 | Benzene | |
| Hexanes | 0.03 | Toluene | |
| Heptanes | 0.02 | Xylenes | |
| Octanes | | Ethyl Benzene | |
| | | Styrene | |
| | | Indene | |
| | | Napthalene | |
| | | TOTAL | 100.0 |

Calc. H. V., Btu SCF _____  Air Content _____

Calc. sp gr (Air 1.000) _____  Approved by _____

Because the central peak of the radial NO concentration profile closely resembled the methane profile and because the maximum NO concentration occurred in one of the "coldest" regions in the flame, the NDIR analyzer was investigated for possible optical interference between NO and another molecule in the gas sample.

We discovered that ethylene ($C_2H_4$) and propylene ($C_3H_6$) would optically interfere with the optical analysis of NO concentrations by the NDIR technique. The intensity of the interference was measured as 100 ppm of ethylene ($C_2H_4$), indicating a 2.1 ppm concentration of NO, and 100 ppm of propylene ($C_3H_6$) being analyzed as 1.1 ppm of NO. This analysis indicated that a correction for the NO data must be applied to measurements made in regions of high hydrocarbon concentrations. (A complete discussion of the correction method is given later in this report.) The measured profile, when corrected (Figure I-14), is very similar in shape to that of the corresponding temperature profile, Figure I-13.

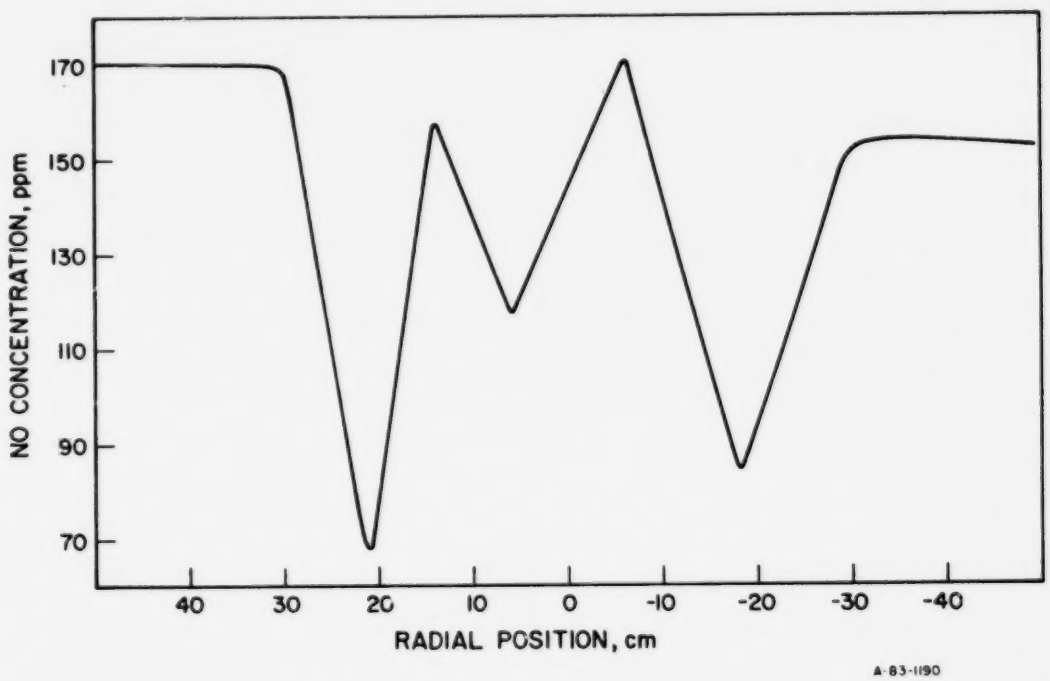


Figure I-14. RADIAL PROFILE FOR NO CONCENTRATION FOR THE SHORT-FLAME BAFFLE BURNER USING THE AXIAL NOZZLE AT A 7.6-cm AXIAL POSITION. GAS INPUT, 2190 CF/hr; EXCESS OXYGEN, 3.0%; PREHEATED AIR, 315°F

The "hot" regions (2680°F and 2870°F) of the flame occur at +15 and −15 cm while the radial position of +15 and −6 cm correspond to the two maximum internal inflection points of the NO profile.

Movable-Block Swirl Burner (I. F. R. F. Design)

Figure I-15 shows the design of the movable-block swirl burner. The fuel gas is introduced through a 3/4-inch pipe along the axis of the burner. The combustion air enters perpendicular to the axis of the burner, passes through an array of swirl generating blocks, and exits into a 0-degree angle burner block with a 7.6-cm radius. The swirl generating blocks are arranged as shown in Figure I-16. There is a total of sixteen blocks; eight are fixed to the burner, and the remaining eight are mounted on a movable plate. If the plate is positioned in its maximum clockwise rotation, the tangential entry channels are completely blocked. Thus, the combustion air has only an axial velocity component. However, if the plate is positioned at its maximum counterclockwise rotation, the air can enter only through the tangential channels. If the movable blocks are adjusted to some intermediate position, the combustion air enters with some combination of axial and tangential velocity components.

The swirl burner was operated at three different swirl intensities for the input-output tests, with two gas nozzle positions for each swirl intensity. For the first gas nozzle position, the nozzle tip was located even with the inside edge of the burner wall (hot face), while in the second position the nozzle tip was withdrawn into the burner block, 6 inches from the hot face wall. (For the remainder of this report, these positions will be referred to as the "exit position" and "throat position," respectively.) The input-output tests were conducted at gas inputs of 1578, 1976, and 2382 CF/hr, with between 10 and 80% of excess air.

The input-output data from the movable-block swirl burner showed the following:

- The maximum measured NO concentration occurred at the lowest levels of gas input (1578 CF/hr) and swirl density.
- At excess oxygen levels below 6%, generally more NO was formed when the gas nozzle was in the throat position than when it was in the exit position. Insufficient data are available to evaluate the relative effect of burner nozzle position when operating with more than 6% excess oxygen.

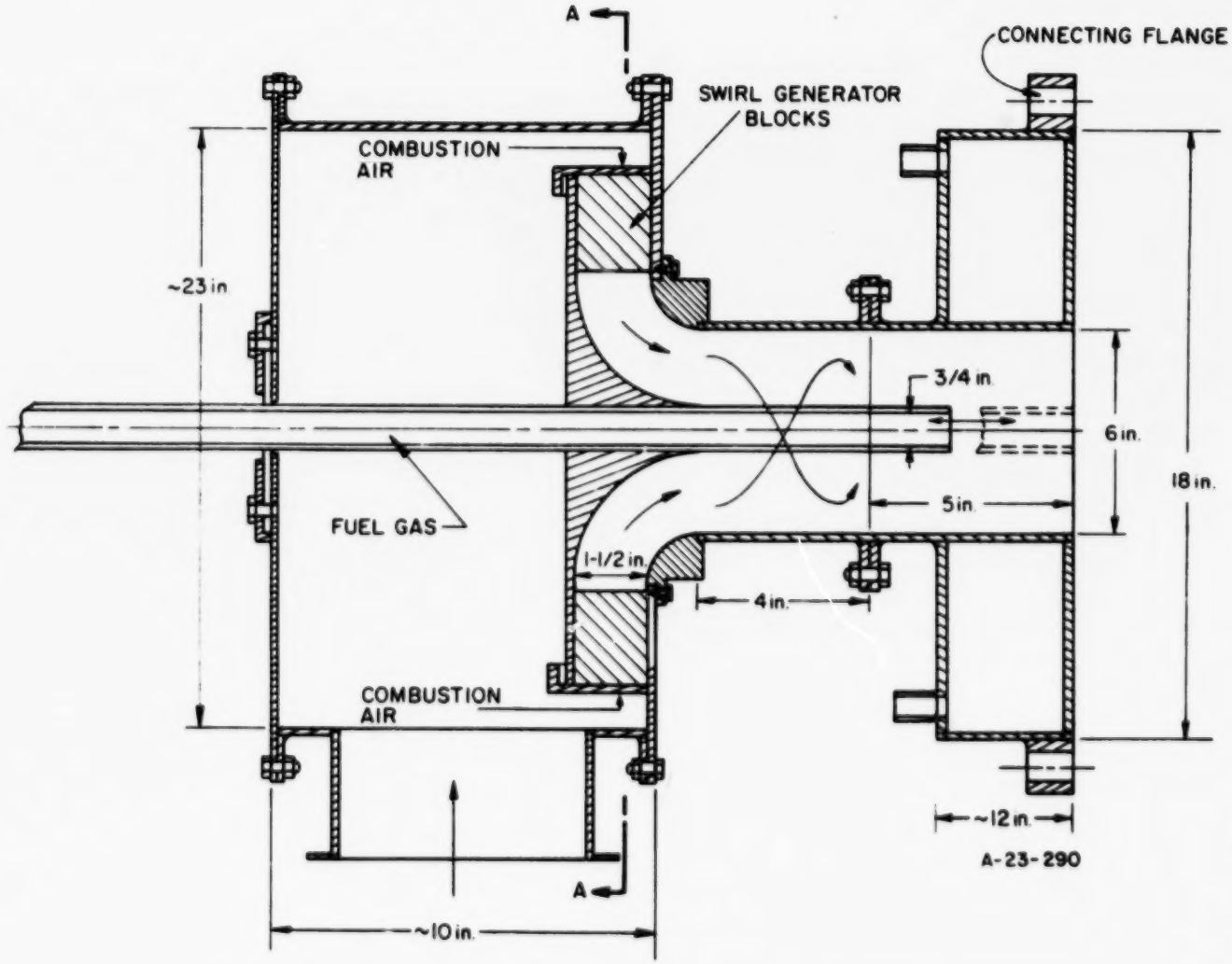


Figure I-15. DIAGRAM OF A MOVABLE-BLOCK SWIRL BURNER

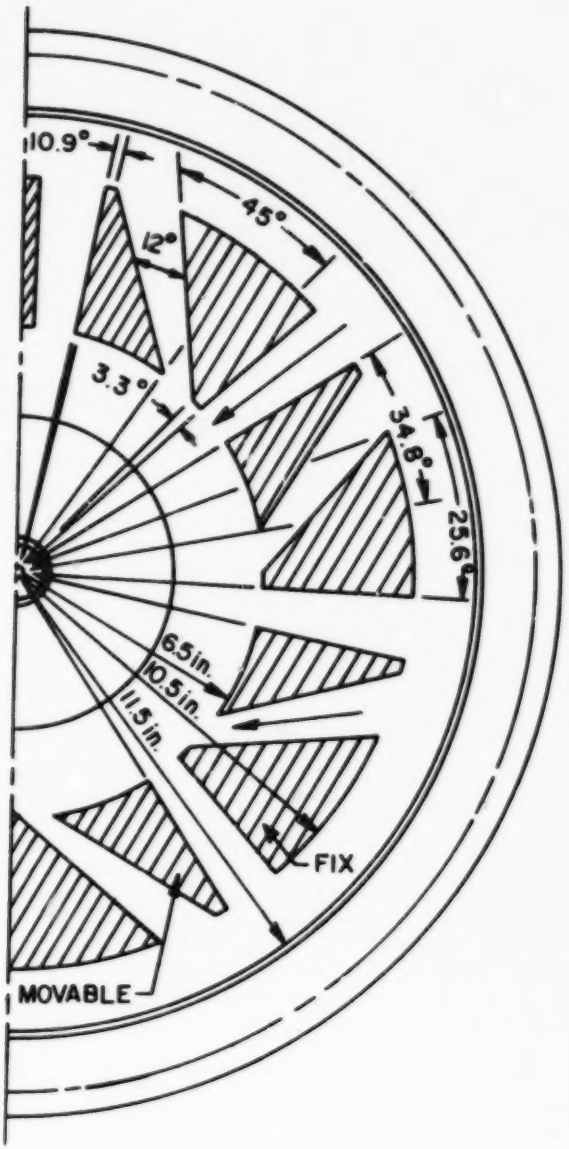


A-23-291

Figure 1-16. ARRANGEMENT OF SWIRL GENERATING BLOCKS IN THE MOVABLE-BLOCK SWIRL BURNER

- Increasing gas input (and consequently gas velocity) always reduced the normalized concentration of NO independent of swirl intensity and percent excess air, when the burner was in the throat position. However, when the nozzle was in the exit position, changing gas input had little or no effect on the normalized NO concentration. This was observed for intermediate and high swirl intensity. Insufficient data were obtainable for the case of low swirl intensity.

Figure I-17 shows normalized NO concentrations as a function of the amount of excess air and the gas nozzle position for high swirl intensity (axial entry channels closed) with a 1976 CF/hr gas input. Figures I-18 and I-19 show normalized NO concentrations as a function of excess air and gas nozzle position for intermediate and low swirl intensities.

A comparison of Figures I-17, I-18, and I-19 at 8-22% excess air (the region of practical interest) discloses several observations concerning the effect of swirl on NO production. For the throat and exit gas nozzle positions, the minimum NO concentration (76 and 34 ppm) are generated by an intermediate swirl intensity with 2% excess oxygen. Intermediate swirl intensity also produces the maximum NO concentrations of 146 ppm with the gas nozzle in the throat position and 82 ppm with the nozzle in the exit position at an excess air level of 22%. Normalized NO concentration profiles as a function of swirl intensity and excess air are shown in Figure I-20 for the nozzle in the exit position and in Figure I-21 for the nozzle in the throat position.

Figure I-22 displays the radial NO concentration profile at a 12.7-cm axial position for intermediate swirl intensity with the gas nozzle in the throat position. The data were collected at a gas input of 2008 CF/hr with 3.6% oxygen in the flue and no air preheat ($100^0$F).

The NO profile corrected for the optical interferences of ethylene and propylene is presented in Figure I-23. The corrected data are represented on the NO transparency (Figure I-37) by the dashed line. As was the case for the "short" flame baffle burner, the corrected NO profile is similar in shape with the temperature profile. The "hot" regions of the flame ($2309^0$F) occur at +11 and −5 cm while the radial position of +11 and −4 cm correspond to the internal peaks in the NO concentration profile.

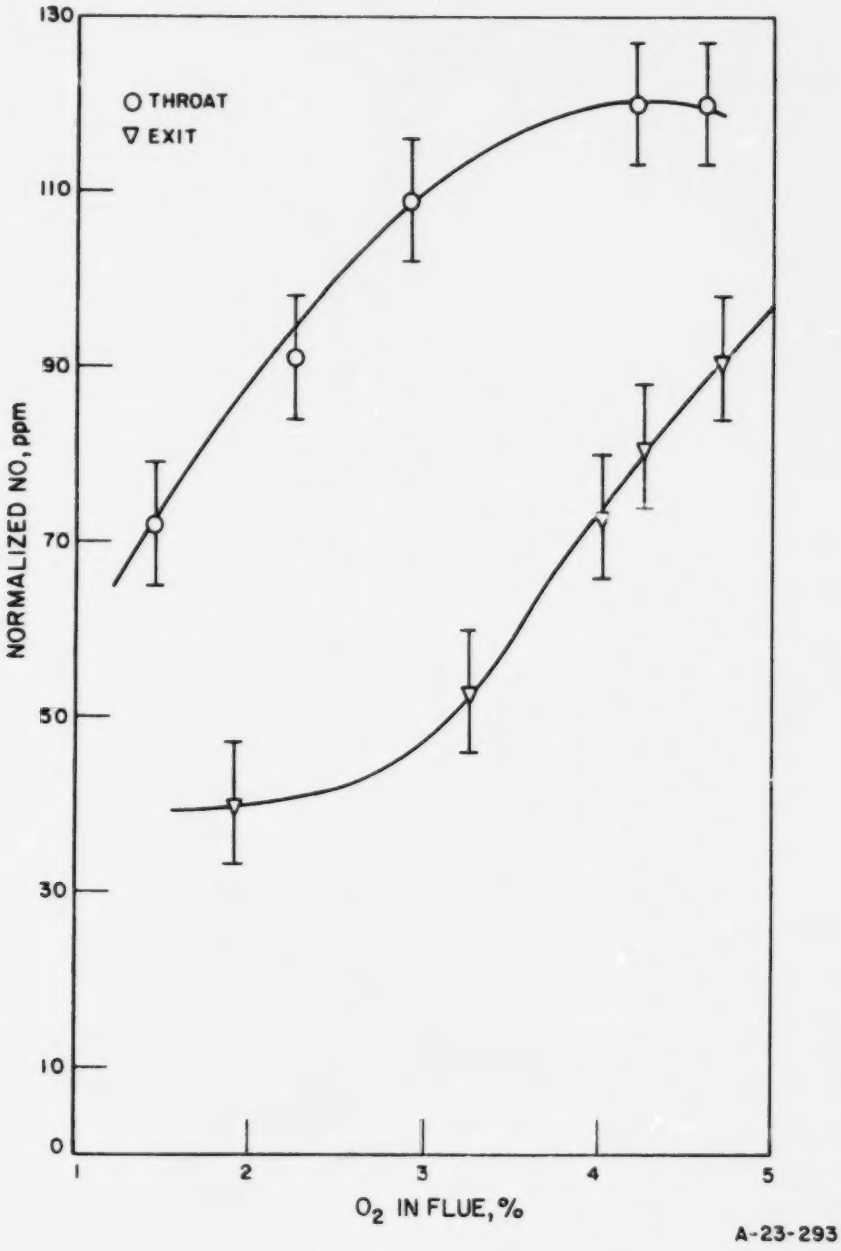


Figure I-17. NORMALIZED NO CONCENTRATION AS A FUNCTION OF EXCESS AIR (Movable Block Swirl Burner – High Swirl Intensity – Gas Input, 1976 CF/hr)

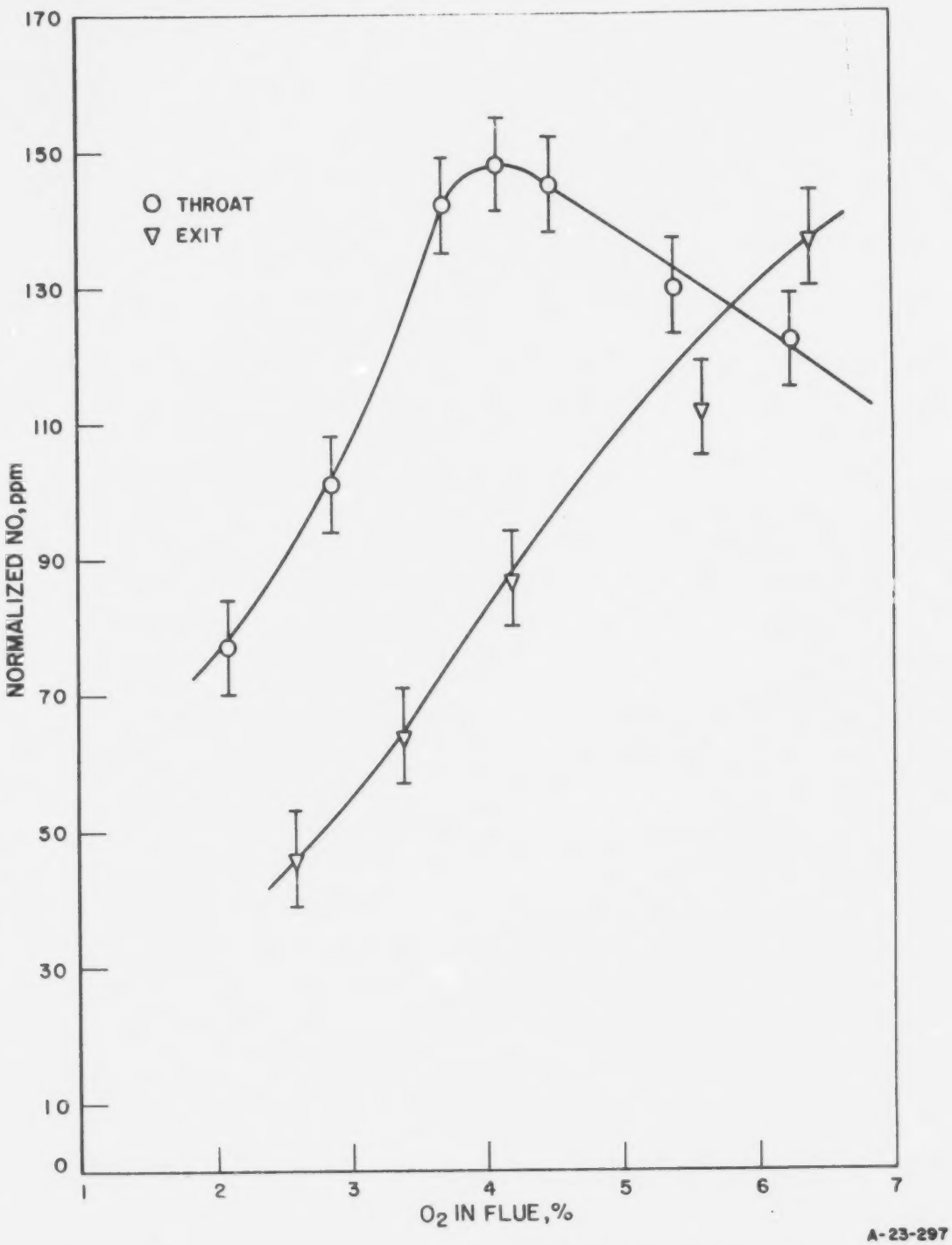


Figure 1-18. NORMALIZED NO CONCENTRATION AS A FUNCTION OF EXCESS AIR (Movable-Block Swirl Burner – Intermediate Swirl Intensity – Gas Input, 1976 CF/hr)

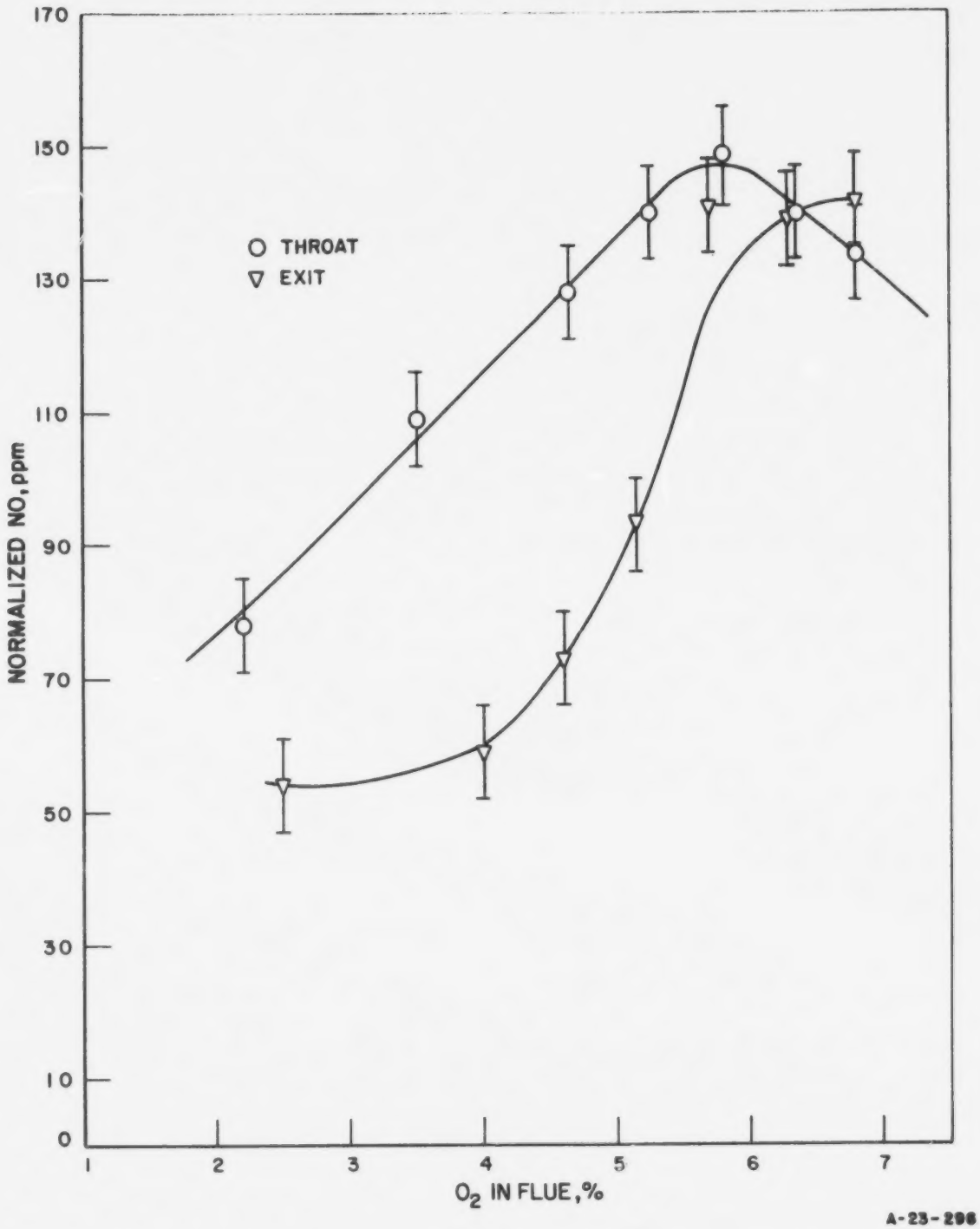


Figure I-19. NORMALIZED NO CONCENTRATION AS A FUNCTION OF EXCESS AIR (Movable Block Swirl Burner – Low Swirl Intensity – Gas Input, 1976 CF/hr)

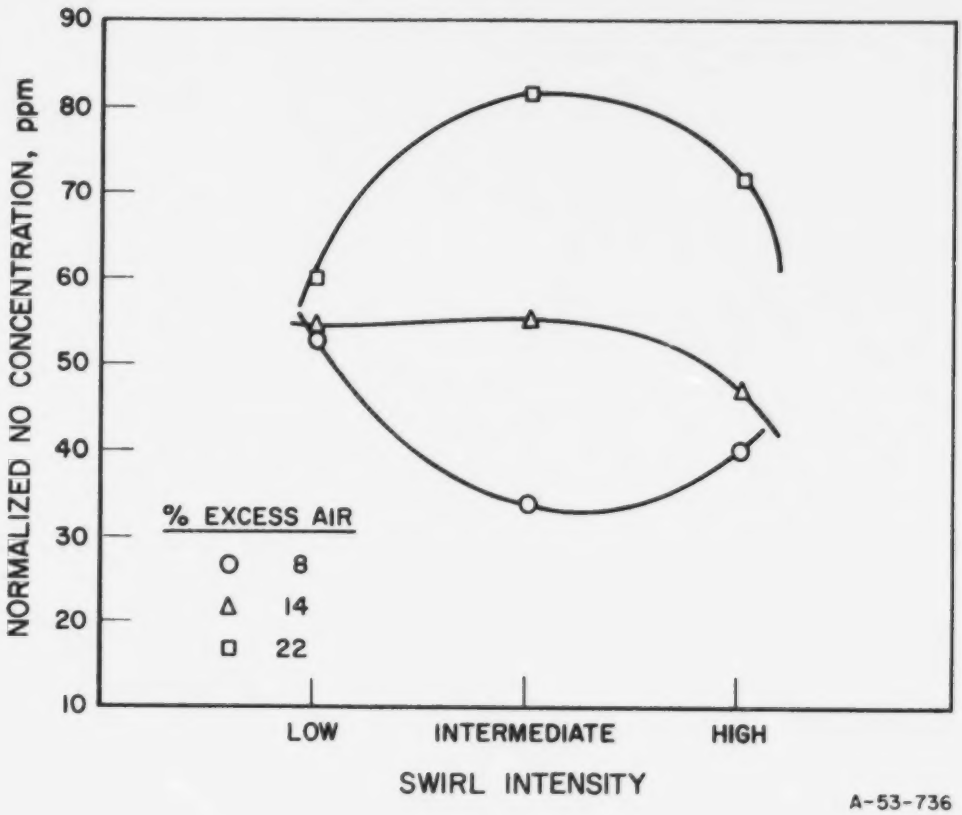


Figure I-20. NORMALIZED NO CONCENTRATION PROFILES AS A FUNCTION OF SWIRL INTENSITY AND EXCESS AIR ON THE MOVABLE-BLOCK SWIRL BURNER WITH GAS NOZZLE IN THE EXIT POSITION

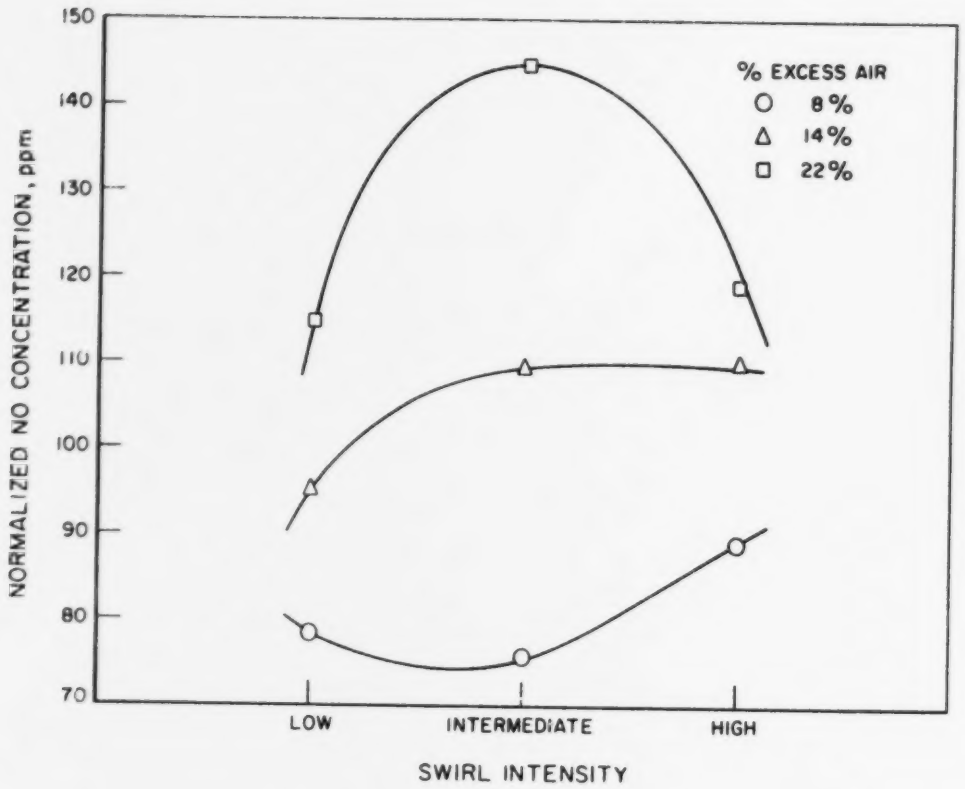


Figure I-21. NORMALIZED NO CONCENTRATION PROFILES AS A FUNCTION OF SWIRL INTENSITY AND EXCESS AIR ON THE MOVABLE-BLOCK SWIRL BURNER WITH GAS NOZZLE IN THE THROAT POSITION

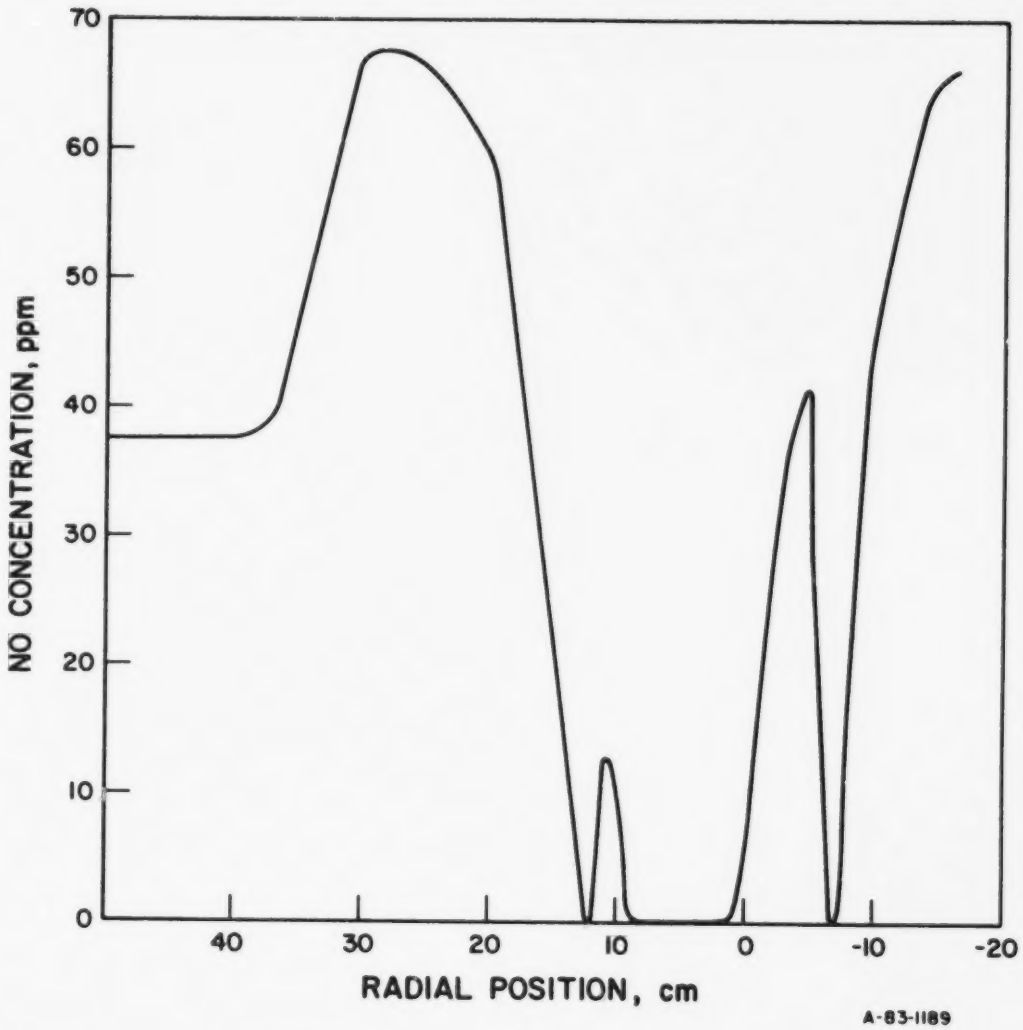


Figure I-22. RADIAL PROFILE OF NO CONCENTRATION AT THE 12.7-cm AXIAL POSITION FOR THE MOVABLE-BLOCK SWIRL BURNER WITH INTERMEDIATE INTENSITY. GAS INPUT, 2008 CF/hr; EXCESS OXYGEN, 3.6%; NOZZLE IN THROAT POSITION

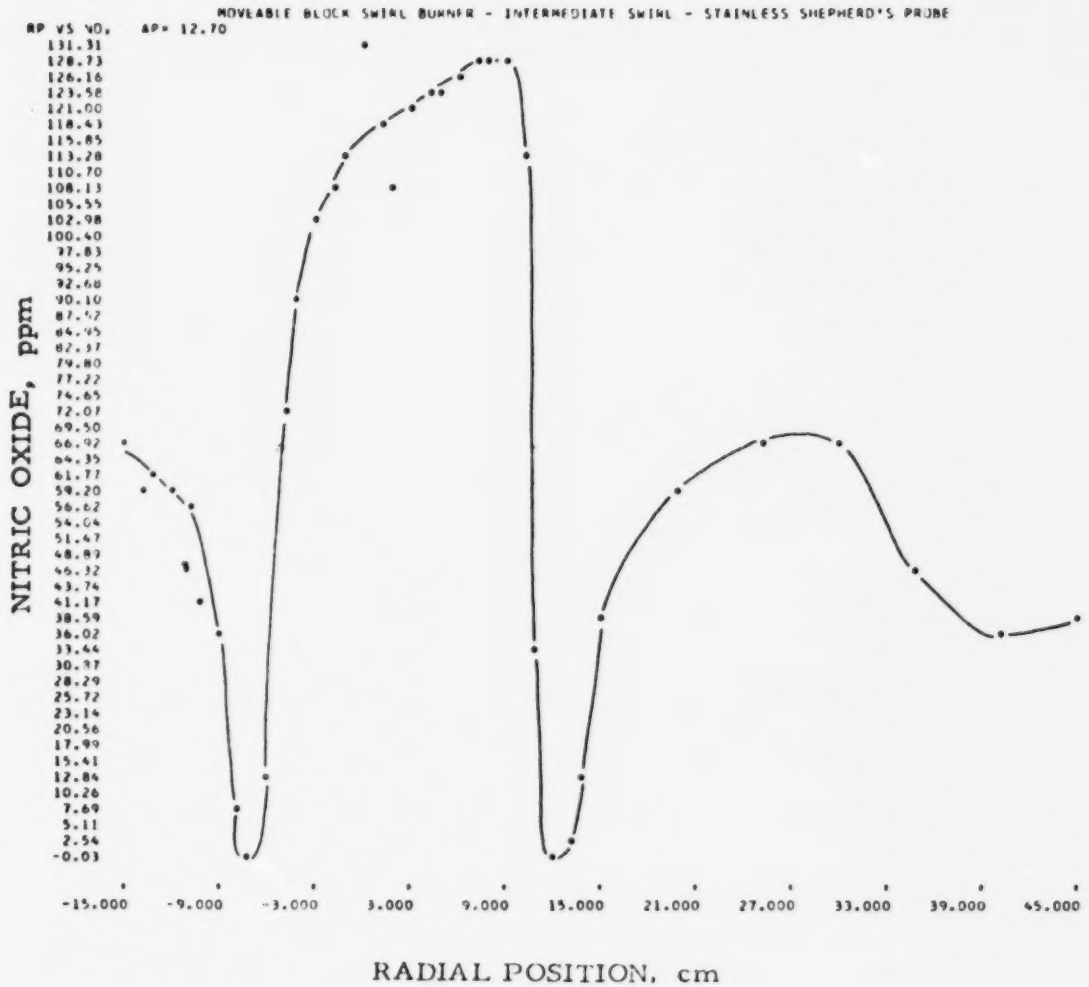


Figure I-23. RADIAL NO CONCENTRATION PROFILE FOR THE MOVABLE-BLOCK BURNER AT AN AXIAL PROBE POSITION OF 12.7-cm AND SET FOR INTERMEDIATE SWIRL INTENSITY, GAS NOZZLE IN THROAT POSITION, 3.6% EXCESS OXYGEN, AND A GAS INPUT OF 2008 CF/hr

The radial temperature profile at the 12.7-cm axial position is shown in Figure I-24. The methane central "cold" spot occurs at a 3-cm radial position. The combustion-air "cold" spots correspond to radial positions of −6 and +13 cm with 15.2 and 15.9% concentrations of oxygen, respectively. The maximum temperatures are measured at +11 and −1-cm radial positions, while the stoichiometric ratios of fuel and air occur at +11.5 and −5.5 cm.

A visualization of these variations in temperature, velocity, $O_2$, $CH_4$, and NO as a function of radial position at the 12.7-cm axial position can be aided by the accompanying transparencies.

To investigate the presence of higher hydrocarbons in the flame, a grab sample was taken at the −1.0-cm radial position and a 12.7-cm axial position. This sample was analyzed using a mass spectrometer and the results are listed in Table I-4. In addition to the ethylene and acetylene which were measured for both the axial burner "short" flame baffle (Table I-2) and the movable-block swirl burner (Table I-4), the swirl burner also produced 0.2 mol % of propylene.

Flat-Flame Burner

When penetration of the flame into the furnace is not desired, a flat-flame burner can be used. Figure I-25 illustrates a partial cutaway view of a nozzle mixing burner of this type. The flat-flame or high-intensity burner actually heats its own refractory burner block tile and the refractory surface of the surrounding furnace wall, primarily by convection, from the high-velocity combustion gases thrown sideways from the burner. These hot refractory surfaces then radiate heat to the furnace load. Because the hot gases have no final velocity component along the burner axis, an extreme case of Type II flame pattern results.

The flat-flame burner was operated at three different gas inputs, all over a range of fuel/air ratios expressed as percentage of oxygen in the flue. No changes were made in the burner nozzle position or the swirl vanes in the burner housing because these were fixed by design. The

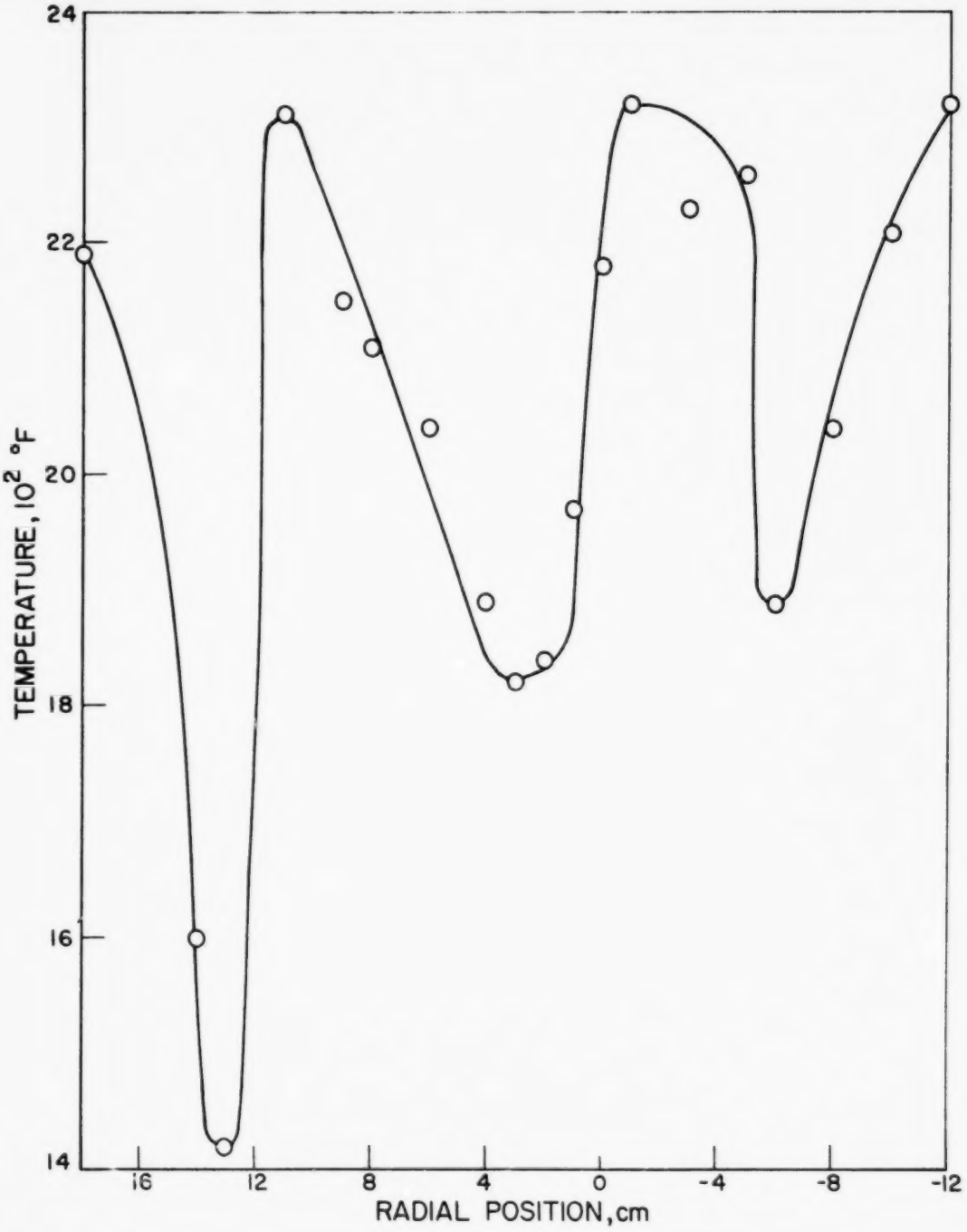


Figure I-24. RADIAL TEMPERATURE PROFILE AT THE 12.7-cm AXIAL POSITION (Movable-Block Swirl Burner – Intermediate Flame Intensity – Nozzle in Throat Position – Gas Input, 2008 CF/hr – 3.6% Excess Oxygen)

Table I-4.

**MASS SPECTROMETER LABORATORY**
**ANALYTICAL REPORT**

Material 8933 Furnace Product Gas
Radial Position, -1 cm; Axial Position, 12.5 cm

Date 1/11/73

Requested by _____

M. S. Run No. 3554

| | Mol % | | Mol % |
|---|---|---|---|
| Nitrogen | 51.7 | Ethylene | 0.4 |
| Carbon Monoxide | 3.2 | Propylene | 0.2 |
| Nitrogen+CO | | Butenes | |
| Oxygen | 2.8 | Pentenes | |
| Carbon Dioxide | 3.8 | Hexenes | |
| Hydrogen | 4.0 | | |
| Argon | 0.6 | 1,3-Butadiene | |
| Water Vapor | | Pentadienes | |
| Helium | | Cyclopentadiene | |
| Methane | 31.8 | Acetylene | 0.4 |
| Ethane | 1.0 | Diacetylene | |
| Propane | 0.1 | Methyl Acetylene | |
| n-Butane | | +Propadiene | |
| Isobutane | | Vinyl Acetylene | |
| Pentanes | | Benzene | |
| Hexanes | | Toluene | |
| Heptanes | | Xylenes | |
| Octanes | | Ethyl Benzene | |
| | | Styrene | |
| | | Indene | |
| | | Napthalene | |
| | | TOTAL | 100.0 |

Calc. H. V., Btu SCF _____

Calc. sp gr (Air 1.000) _____

Air Content _____

Approved by _____

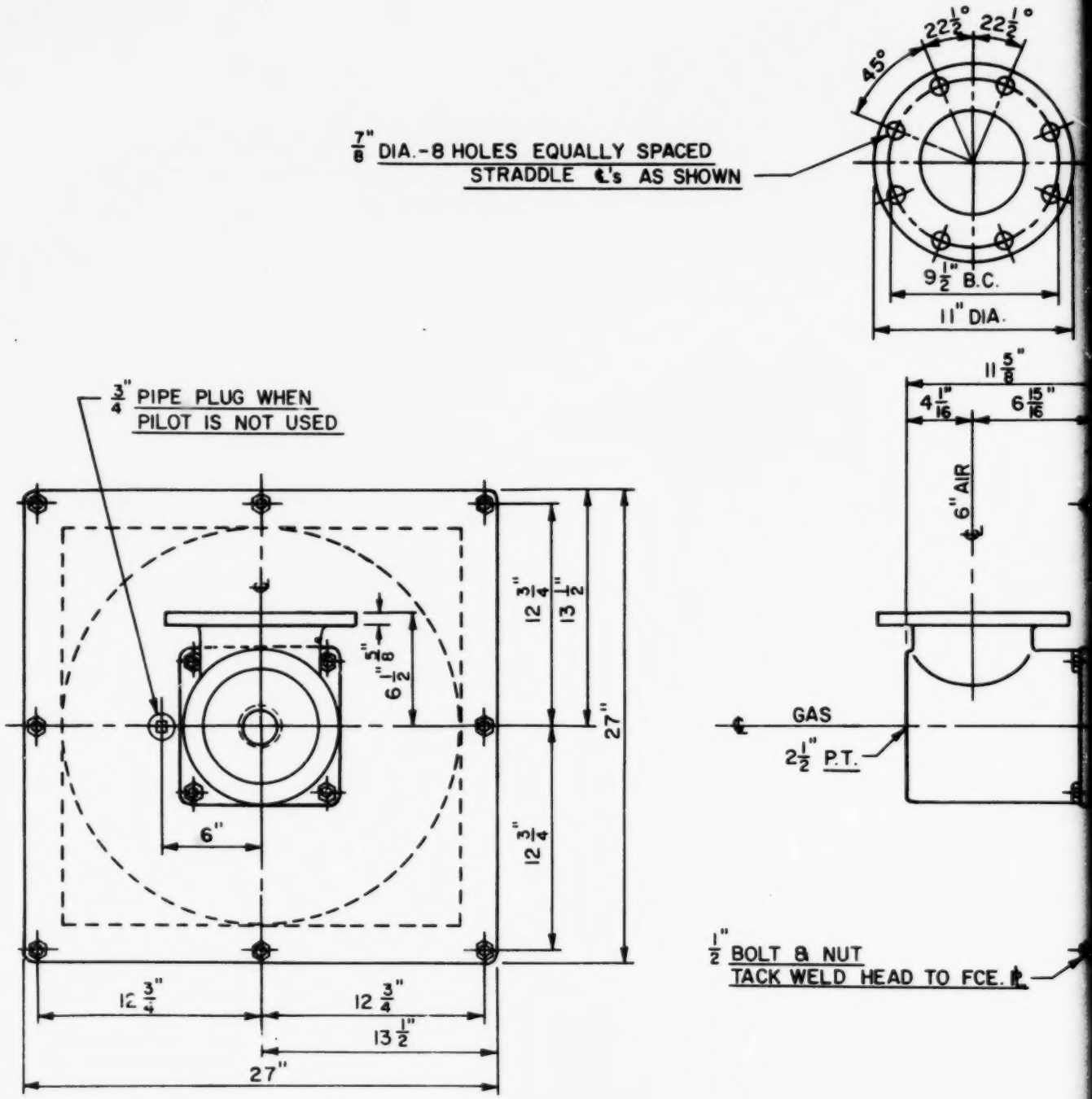


A-5

Figure I-25. CROSS-SECTIONAL VIEW OF THE FLAT FLAME HIGH-INTE

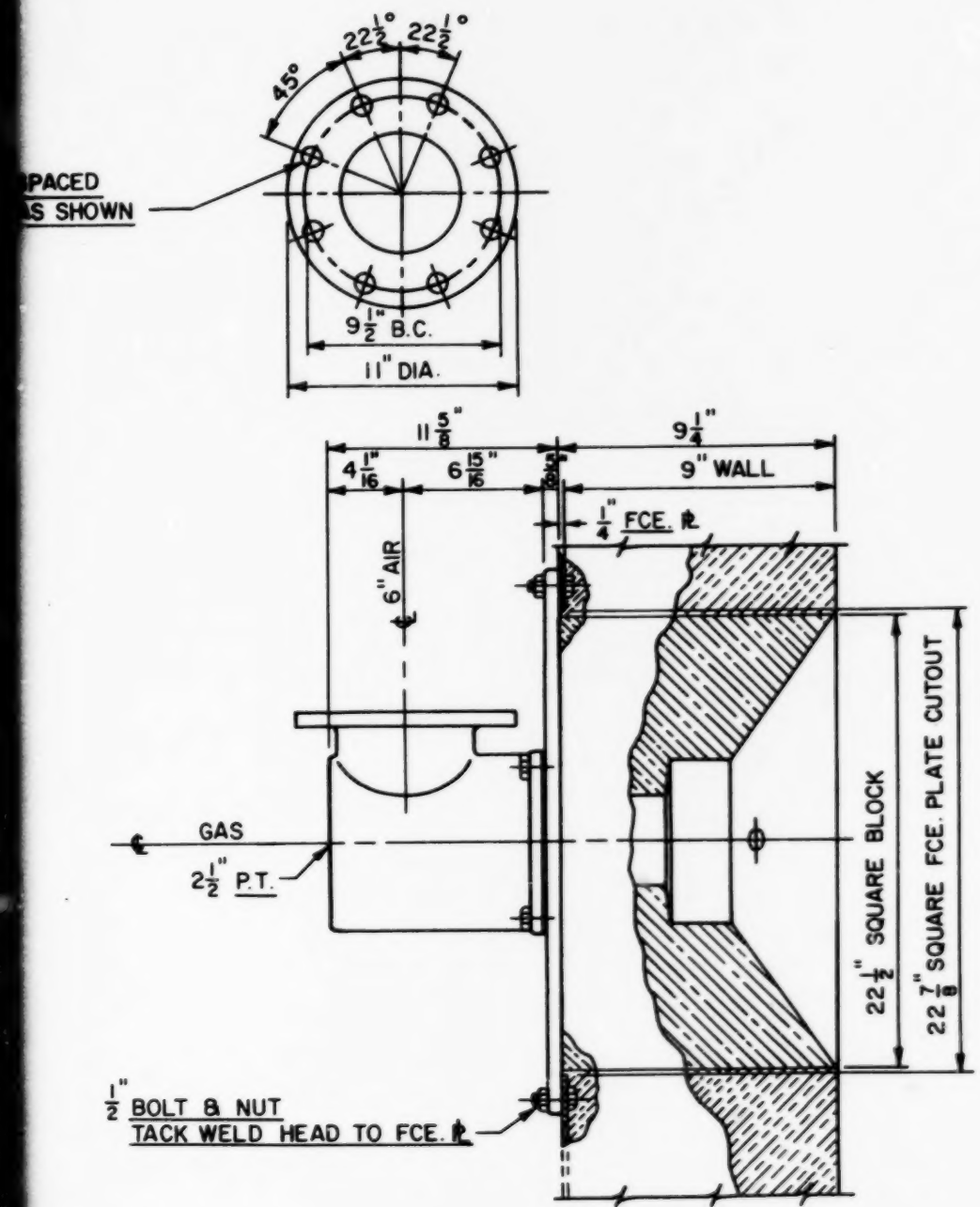


A-53-788

W OF THE FLAT FLAME HIGH-INTENSITY BURNER

input-output tests were conducted at gas inputs of 1670, 2010, and 2394 CF/hr, with between 1.0 and 7.0% oxygen in the flue by volume.

Figure I-26 shows the normalized NO concentrations measured in the flue as a function of excess air and gas input for the flat-flame burner.

Based on the analysis of the input-output results, we concluded the following:

1. From 1.0 to about 3.75% excess oxygen in the flue, the gas input rate made little difference in the amount of NO formed so long as the flame had a visible appearance of being flat. Spot-check runs for NO in the flue gases at gas inputs below 1670 CF/hr (where the flame lost its flat appearance) showed differences as gas input was changed. However, the flame was very lazy and concentration readings erratic. Definite measurements could not be made, only gross differences observed. Consequently, measurements at gas inputs below 1670 CF/hr were not pursued further.

2. The NO concentration at all gas inputs and excess air levels tested was considerably lower for the flat-flame burner than any other "commercial type" burner tested. As the gas input was increased, the peak NO concentrations decreased in magnitude and occurred at lower percentages of excess oxygen. We postulate that this occurs because at higher inputs the flame is held closer to the burner block and the wall of the furnace. Because of increased heat transfer to these walls, the combustion area is cooled. This cooling effect, in turn, tends to reduce the energy available to the $NO_x$-forming reactions.

The NO concentration radial profile at a 12.7-cm axial position is given in Figure I-27. We observe very little curvature or noticeable shape in this profile; however, an increase occurs in the magnitude of the average NO concentration moving across the furnace from left to right. Hydrocarbon correction of these data was not necessary. The measured data points can be considered to be within the interval concentration level of 74 ppm ± 10. The average concentration of this profile is 77 ppm. As compared with the flue concentration of 88 ppm, this would seem to indicate that most of the NO was formed during the initial combustion processes inside the burner block.

The radial temperature profiles for axial positions of 12.7, 69, and 130 cm are displayed in Figure I-28. At the 12.7-cm axial position, a minimum occurs on the axis of the burner where the main contributions would be caused by recirculating gases. There is only an 80°F difference between this minimum temperature and the maximum temperature which

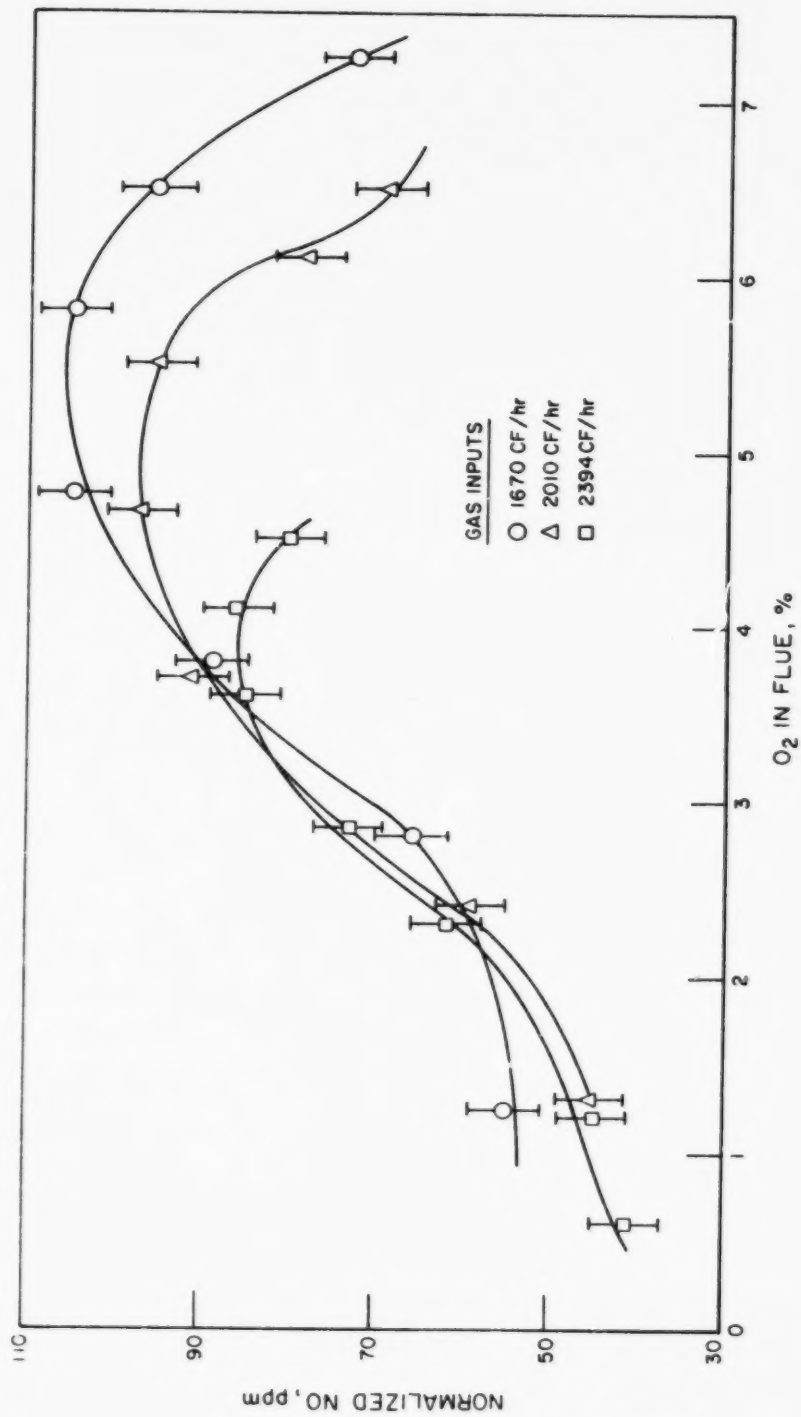


Figure I-26. NORMALIZED NO CONCENTRATION AS A FUNCTION OF EXCESS AIR FOR THE FLAT-FLAME BURNER

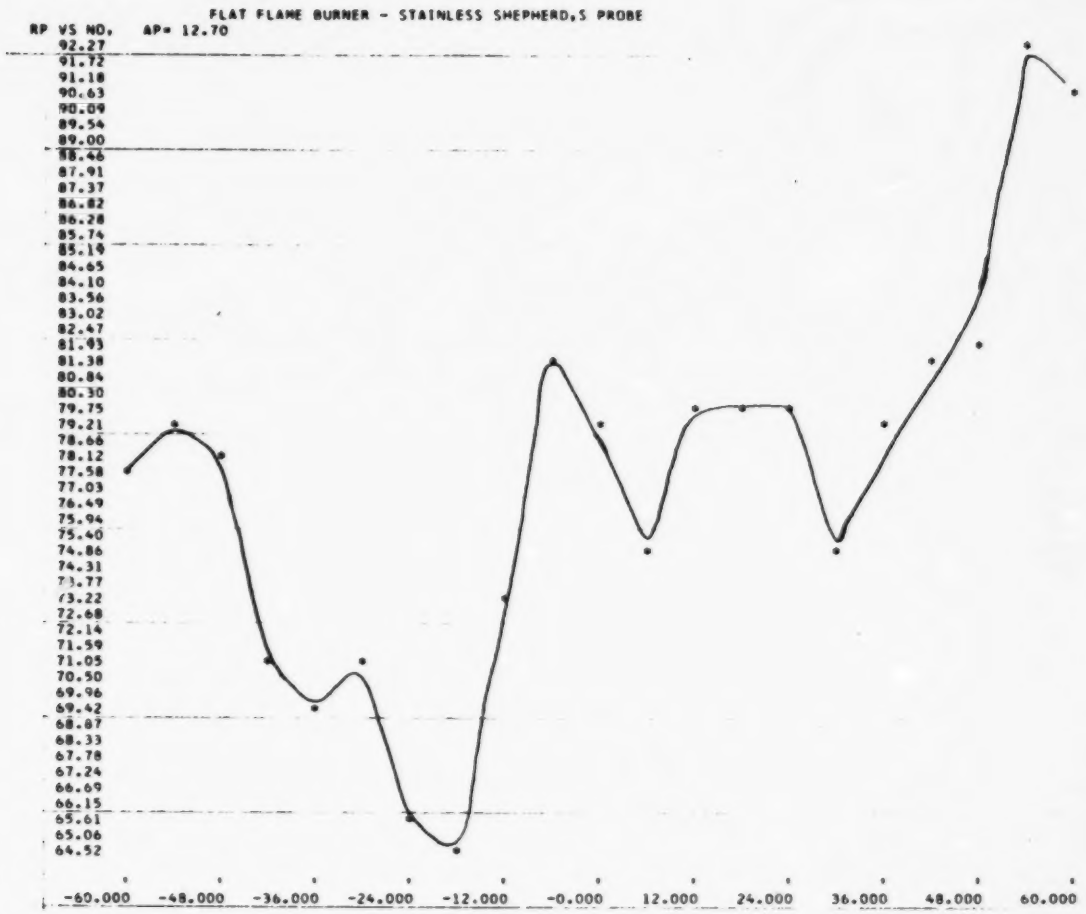


Figure I-27. RADIAL NO CONCENTRATION PROFILE FOR THE FLAT FLAME BURNER AT A 12.7-cm AXIAL POSITION

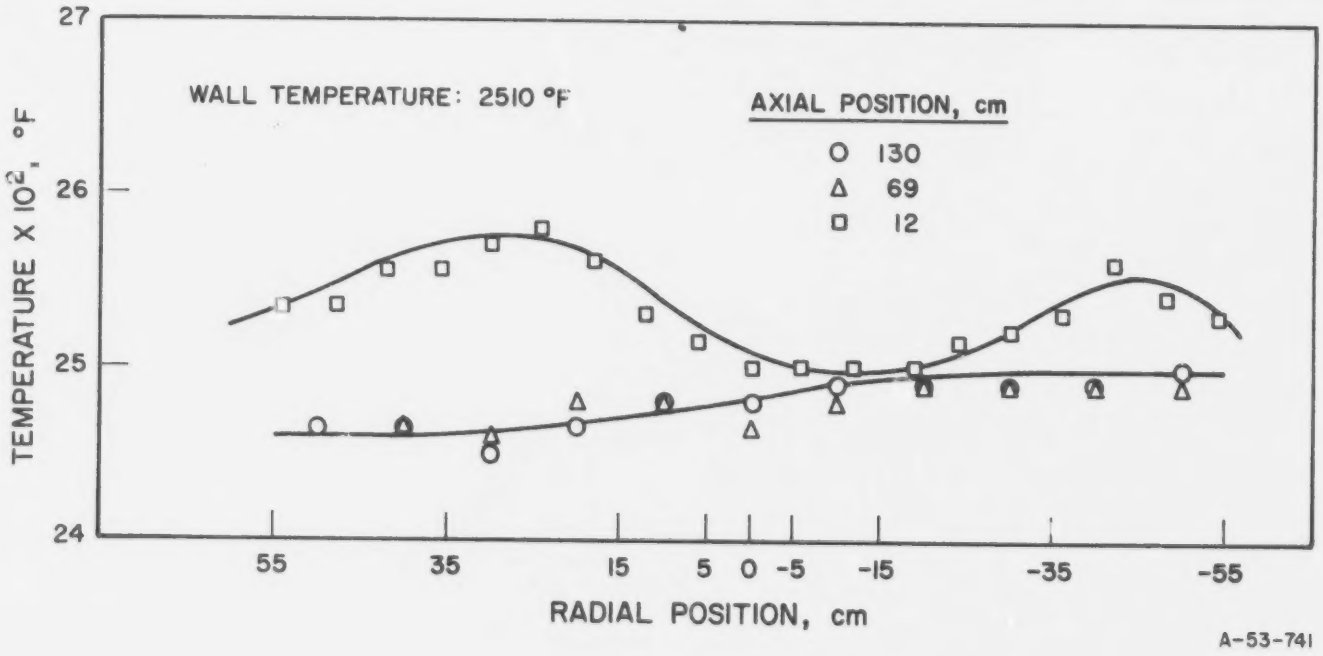


Figure I-28. RADIAL TEMPERATURE PROFILES FOR THE FLAT FLAME BURNER AT AXIAL POSITIONS OF 12.7, 69, AND 130 cm

occurs at a 24-cm radial position. The radial temperature profiles at the 69 and 130-cm axial positions are essentially the same, maintaining a fairly constant value of 2480° ± 20°F.

Boiler Burner

A guide-vane boiler burner is illustrated in Figure I-29. The combustion air enters perpendicular to the axis of the burner and then passes through a register of guide zones which impart a degree of swirl dependent on their orientation before entering the burner block. Figure I-30 illustrates how the angle of the guide vanes is measured. The burner block has a 30-degree divergent angle with a 45-cm diameter exit into the furnace. All the tests presented here were conducted using radial gas injection with a gas throughput of 3040 CF/hr.

Normalized NO concentrations in the flue as a function of excess air, combustion air preheat, and vane-angle setting are given in Figures I-31, I-32, and I-33. In Figure I-31 at a 30-degree vane-angle setting, the NO curves have very little curvature and are similar in intensity to the short-flame baffle burner with the axial gas nozzle (Figure I-11). For a 40-degree vane-angle setting (Figure I-32), there is a large (52%) increase in the magnitude of the peak NO concentration for the 530°F preheat temperature as compared with a 31% increase in peak concentration for the 270°F preheat. Figure I-33 displays the normalized NO concentration in the flue for a 60-degree vane-angle setting. For the 265° and 530°F preheat temperatures, the shape and magnitudes of the NO profiles remain relatively unchanged from those obtained at a 40-degree vane-angle setting. However, for ambient air temperature, the nitric oxide has a positive slope whereas for the 40-degree angle vane it had no slope.

The swirl numbers corresponding to the vane-angle settings investigated during this project are listed in Table I-5.

Table I-5. VANE-ANGLE SETTING VERSUS SWIRL NUMBER FOR BOILER BURNER

| Vane Angle, deg | Swirl Number |
|---|---|
| 30 | 0.52 |
| 40 | 0.71 |
| 60 | 1.22 |

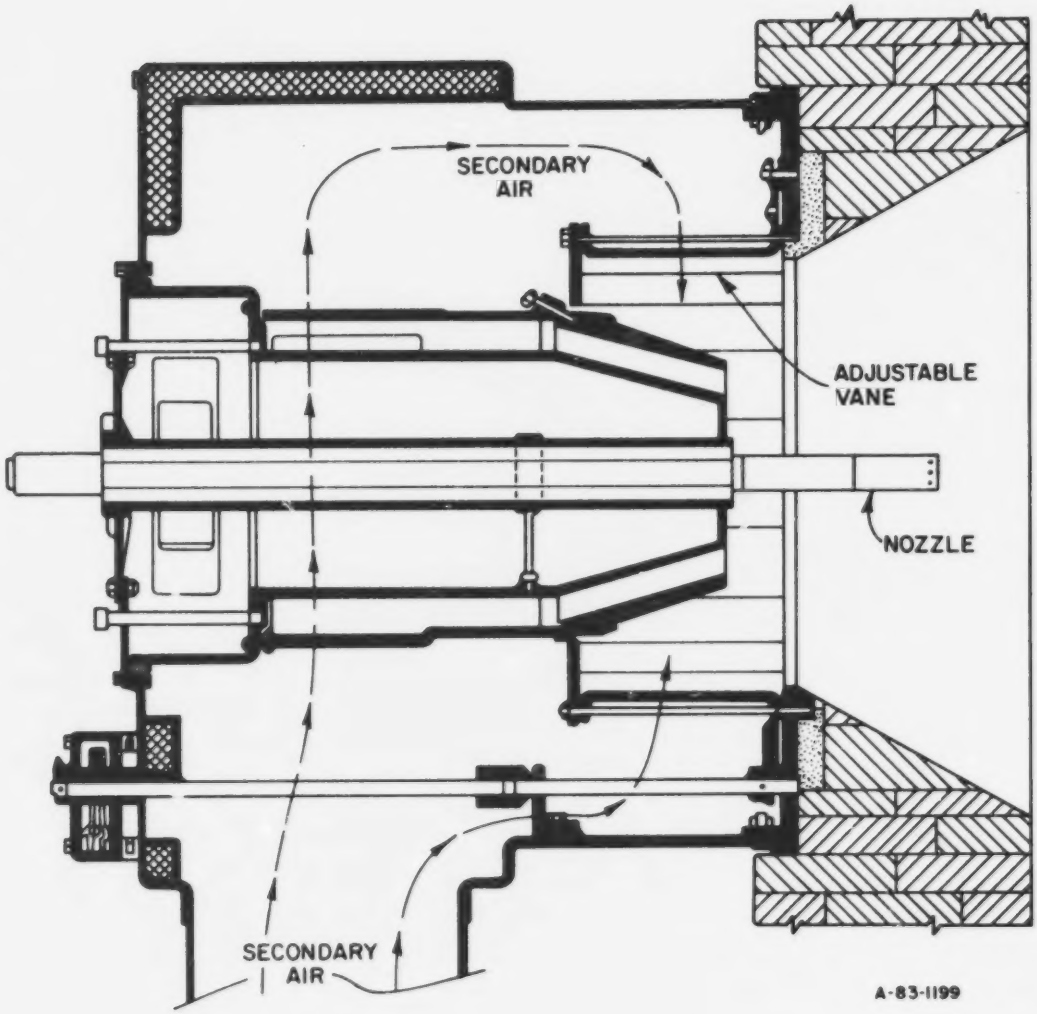


Figure I-29. GUIDE-VANE BOILER BURNER

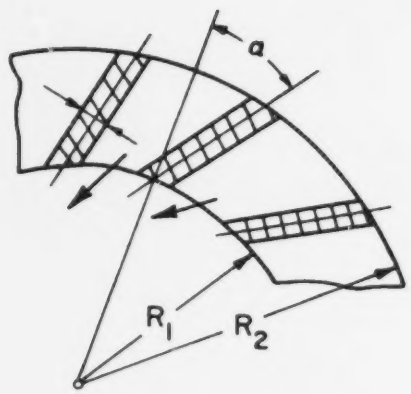


Figure I-30. METHOD OF MEASURING GUIDE VANE ANGLE FOR BOILER BURNER

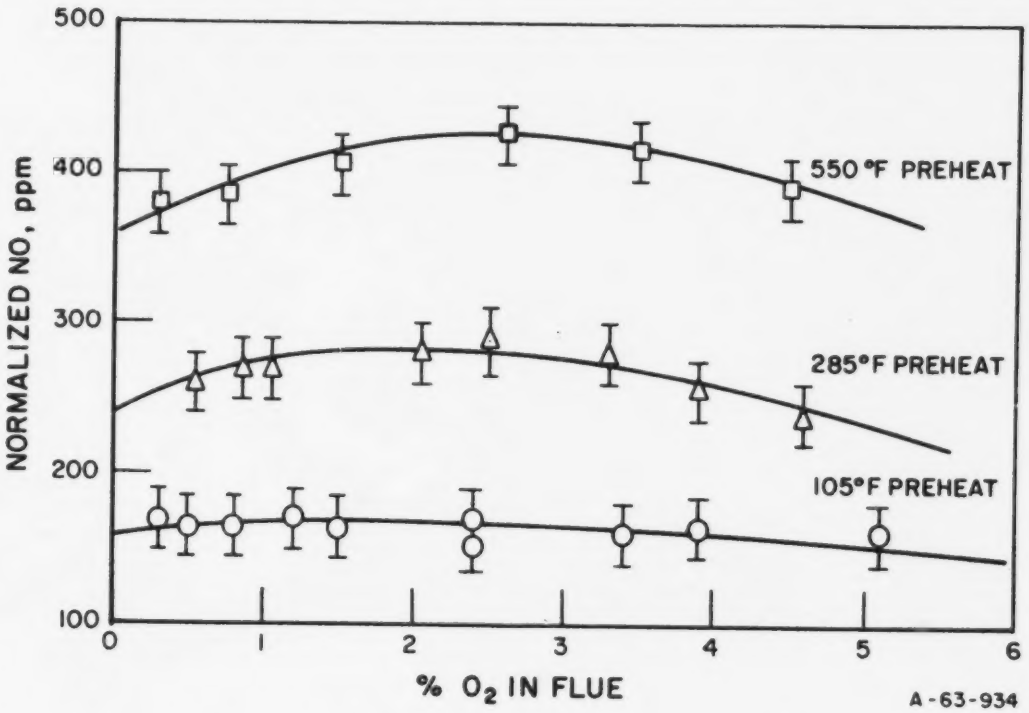


Figure I-31. NORMALIZED NO CONCENTRATION AS A FUNCTION OF EXCESS AIR (Boiler Burner With a 30-deg Angle Vane Setting; Gas Input, 3020 CF/hr)

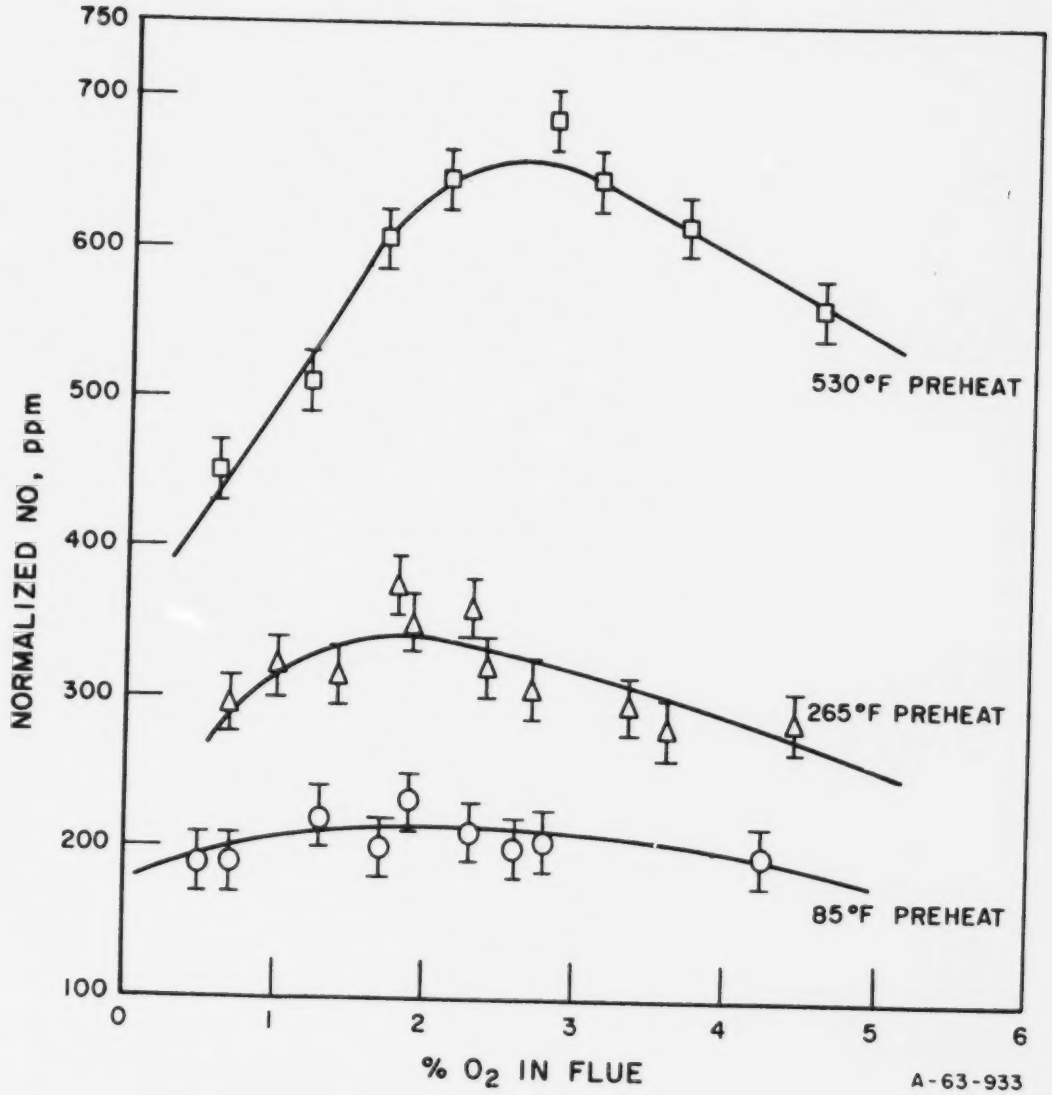


Figure I-32. NORMALIZED NO CONCENTRATION AS A FUNCTION OF EXCESS AIR (Boiler Burner With a 40-deg Angle Vane Setting; Gas Input, 3040 CF/hr)

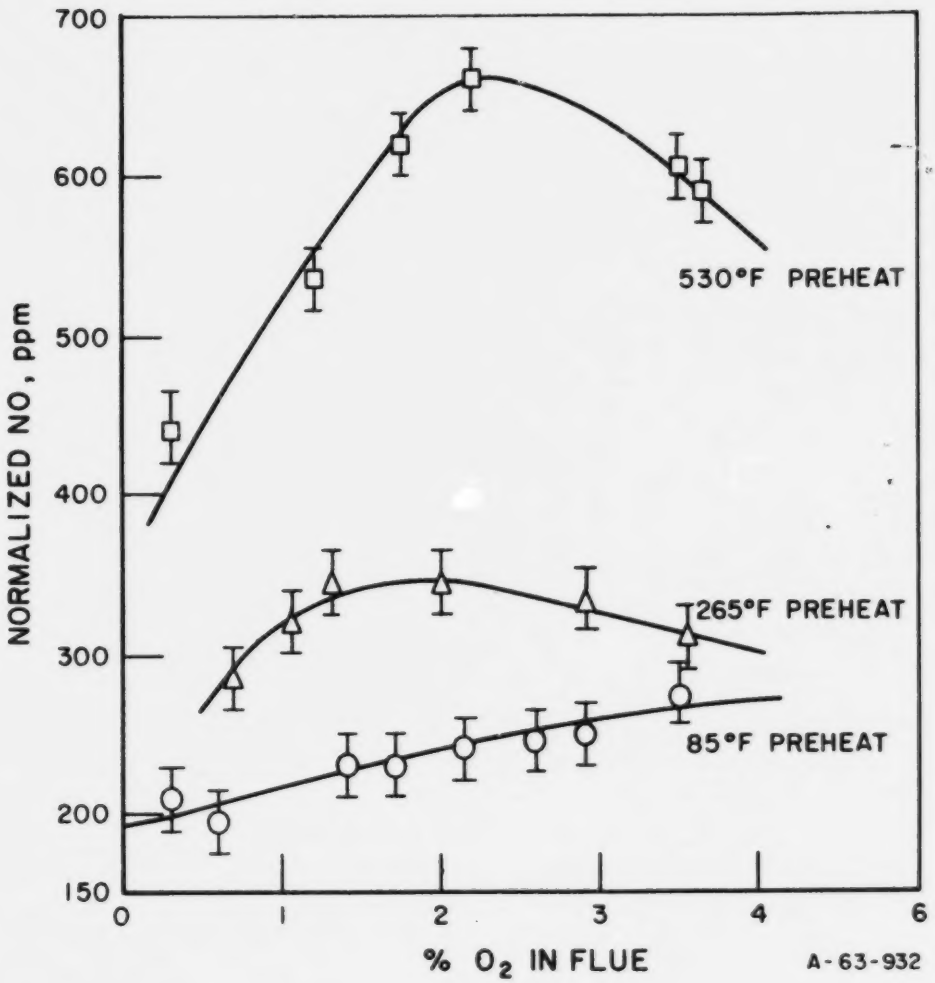


Figure I-33. NORMALIZED NO CONCENTRATION AS A FUNCTION OF EXCESS AIR (Boiler Burner With a 60-deg Angle Vane Setting; Gas Input, 3040 CF/hr)

Figure I-34 presents a set of curves plotting normalized NO concentrations versus swirl number. All the curves were drawn for 2% excess oxygen with each curve representing a different air preheat temperature whose values are labeled. There is no appreciable difference between the curves shown in Figure I-34 and the curves which would represent a 3% excess oxygen level. From Figure I-34 we conclude that the swirl number producing the maximum concentration of NO, independent of the preheated air temperature, would be 1.0. The swirl number corresponds to a 53-deg vane angle.

The radial NO profile is plotted in Figure I-35 for the boiler burner with a 60-deg vane angle setting. These data were collected at a 3039 CF/hr gas input with 8% excess air at a 270$^0$F preheat temperature. On the axis of the burner the measured NO concentration was 242 ppm. The concentration value decreased to a minimum of 136 ppm at a 27-cm radial position and then increased to a rather constant value of 260 ppm in the secondary recirculation zone. A symmetrical distribution of the NO profile would produce a "W"-shaped curve.

The radial temperature profile in Figure I-36 shows a shape characteristic of Type II flames. It has a relatively flat maximum, 2840$^0$F, across the central portion of the burner block, and then falls to a constant temperature of 2560$^0$F in the secondary recirculation zone. The large temperature gradients occur in the region of forward flow out of the burner block, with the maximum temperature plateau corresponding with the internal recirculation zone.

Table I-6 presents a chemical species analysis of a grab sample taken in the furnace at a 12.7-cm axial position and a 30-cm radial position. This radial position was selected because the flame displayed a Type II flow pattern with a region of forward flow within the radial positions of 24 cm and 34 cm. Hydrogen and carbon monoxide were the only combustibles measured. By comparison, the Type I flames, investigated for combustibles within the furnace (Tables I-2 and I-4), not only contained hydrogen and carbon monoxide but also methane, ethane, propane, normal-butane, ethylene, propylene, and acetylene.

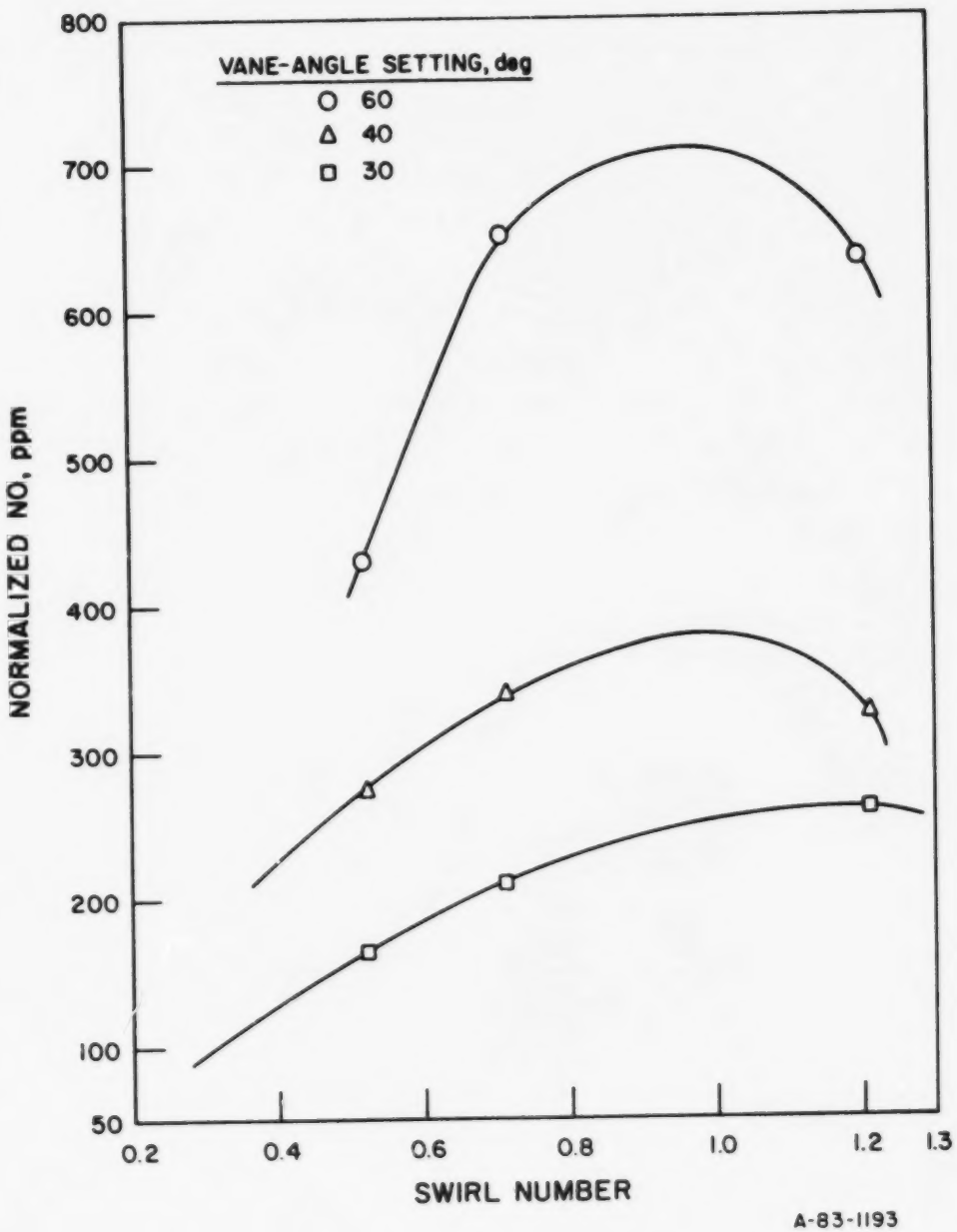


Figure I-34. NO CONCENTRATION VERSUS SWIRL NUMBER

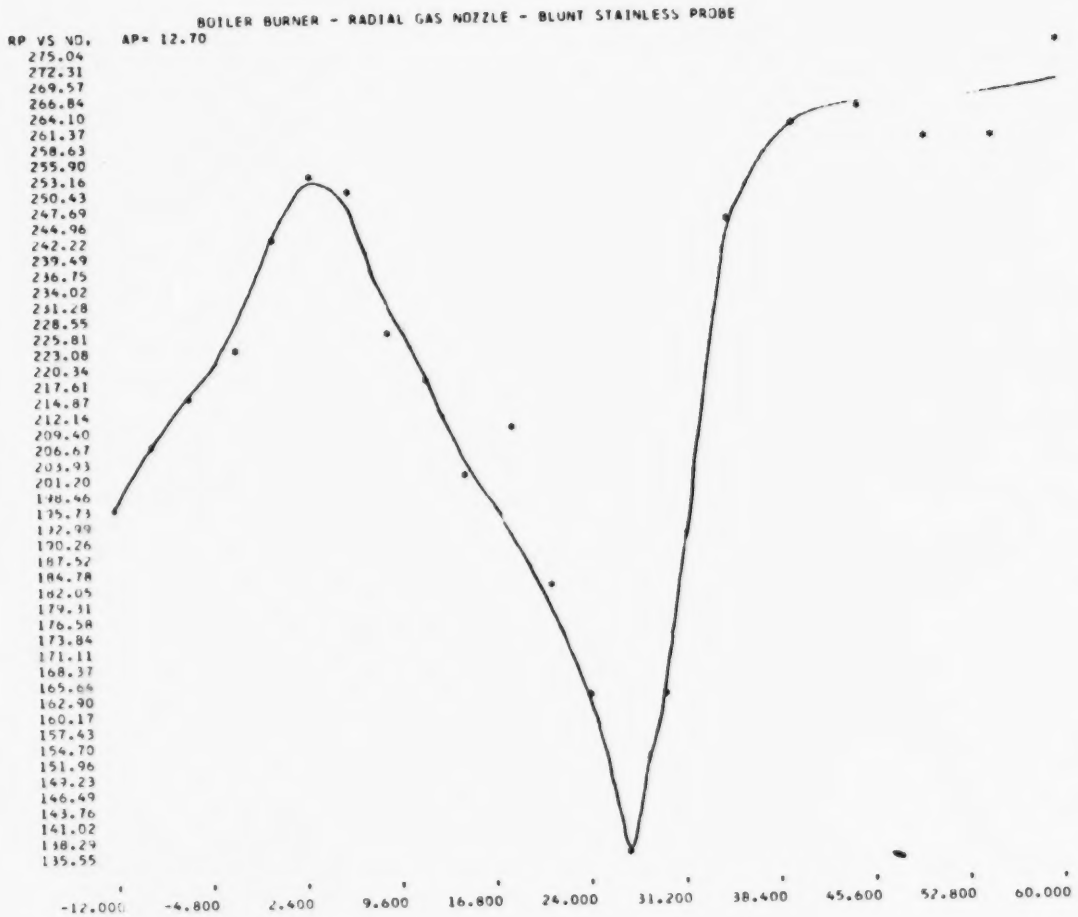


Figure I-35. RADIAL PROFILE FOR NO AT A 60-deg VANE ANGLE SETTING (Boiler Burner – Gas Input, 3039 CF/hr – Preheat Temperature, 270°F – 8% Excess Air)

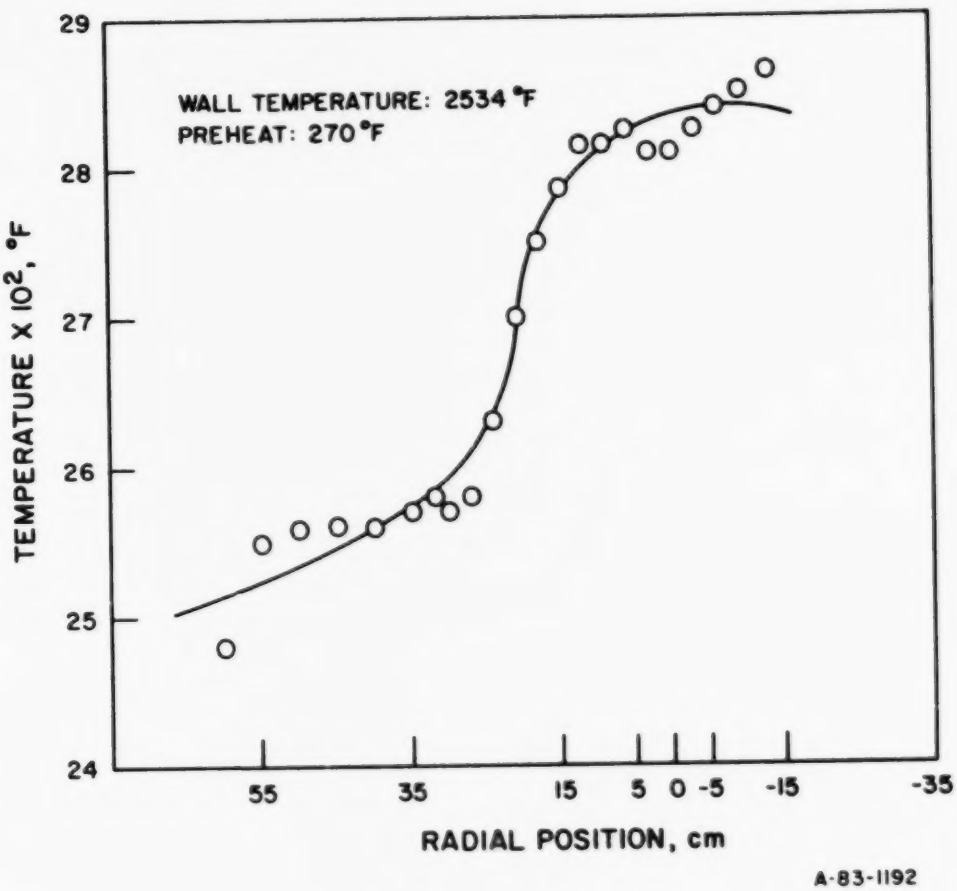


Figure I-36. RADIAL TEMPERATURE PROFILE

Table I-6. MASS SPECTROMETER
LABORATORY ANALYTICAL REPORT

Material: 8933 Furnace Gas Sample  Date: 3/16/73

Requested by: _____  M.S. Run No.: 3875

| | Mol % |
|---|---|
| Nitrogen | 61.3 |
| Carbon Monoxide | 3.3 |
| Oxygen | 0.15 |
| Carbon Dioxide | 6.3 |
| Hydrogen | 2.3 |
| Argon | 0.74 |
| Water Vapor | 25.9 |
| Helium | 0.01 |
| Total | 100.00 |

## GENERAL OBSERVATIONS

Although the "measured" radial profiles of NO concentrations for Type I flames consistently resembled a "W" in shape, with the central inflection point being higher than the two end points, these profiles gave rise to two questions: 1) Why does the central peak in the NO profile closely resemble the methane profile, and 2) why does the maximum NO concentration occur in one of the "coldest" regions of the flame? Both of these situations contradict the work of other investigators. (See Figures I-37 through I-41.)

One possible answer was that of an optical interference within the NDIR analyzer between NO and another molecule in the gas sample being examined. Water has such a strong optical interference with NO. However, being aware of this, we very carefully dried each gas sample before allowing it to enter the analyzer. Before beginning this investigation, dried air, methane, CO, and $CO_2$ were passed through the NO analyzer without detectable interference. However, several molecular species were measured in the flame which had not been investigated for optical interferences. These included ethane, propane, normal-butane, ethylene, propylene, and acetylene as shown in Tables I-3 and I-4. Figure I-42 shows the infrared spectra of these species as well as the infrared spectra of CO, $CO_2$, $CH_4$, NO, and $NO_2$. The lines in Figure I-42 indicate only the location of the center of the infrared bands, but do not represent the width of the bands. The NDIR analyzers used the infrared spectra bands with a wave number of 1876 $cm^{-1}$ for NO, 2143 $cm^{-1}$ for CO, 2350 $cm^{-1}$ for $CO_2$, and approximately 3020 $cm^{-1}$ for $CH_4$. The CO, $CO_2$, and $CH_4$ analyzers have no optical filters and use a quartz window for transmission. Unlike these analyzers, the NO analyzer has a filtering system which passes light within the range of wave numbers 1660 $cm^{-1}$ to 2060 $cm^{-1}$. Figure I-42 indicates that possible optical interferences with the 1876 $cm^{-1}$ NO band are the 1932 $cm^{-1}$ band for $CO_2$, 1936 $cm^{-1}$ band for propane, 1890 $cm^{-1}$ band for ethylene, and the 1830 $cm^{-1}$ band for propylene. To test for optical interference of these bands with the 1876 $cm^{-1}$ band of NO a sample of each gas was measured by the NO analyzer. Only the propylene and ethylene samples indicated any interference. To determine if any of the propylene or ethylene would be

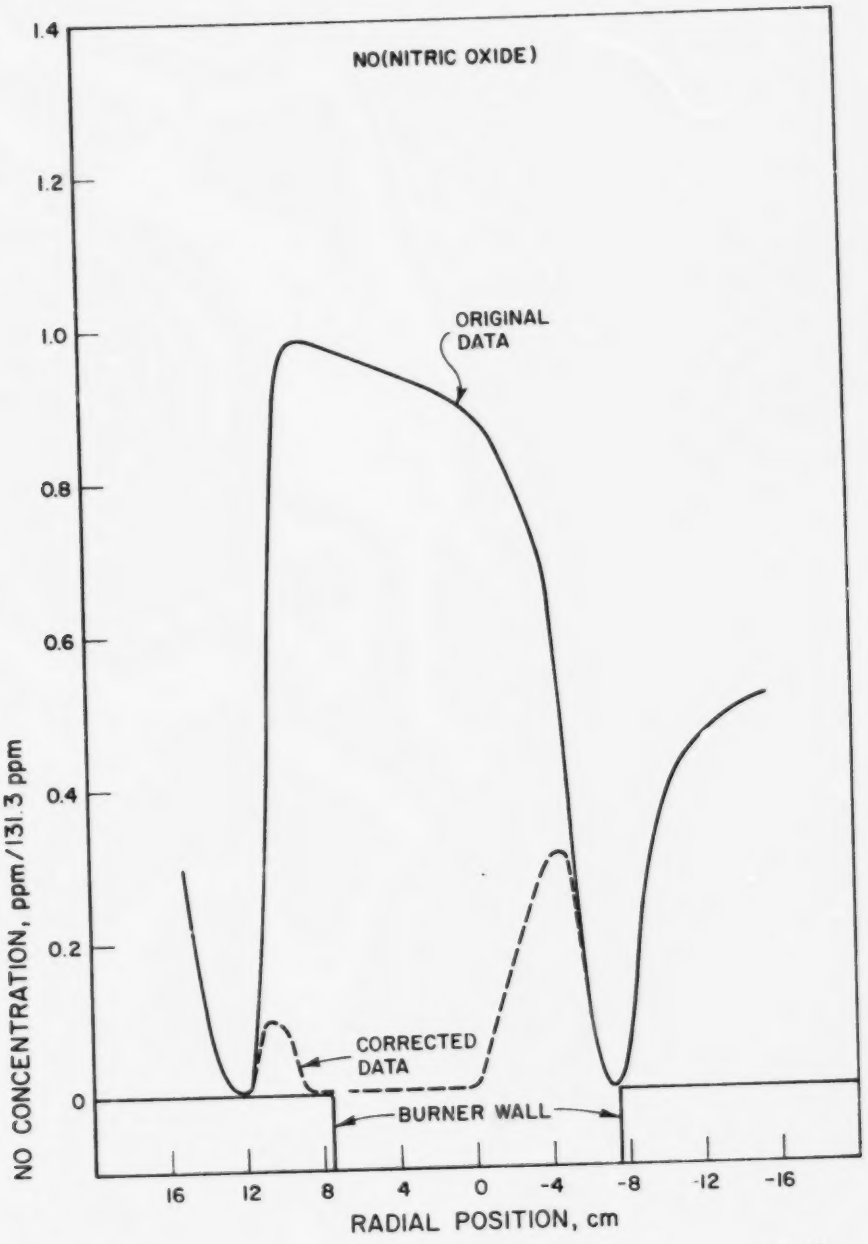


Figure I-37. RADIAL NO CONCENTRATION PROFILE FOR THE MOVABLE-BLOCK BURNER AT AN AXIAL PROBE POSITION OF 12.7 cm AND SET FOR INTERMEDIATE SWIRL INTENSITY, GAS NOZZLE IN THROAT POSITION, 3.6% EXCESS OXYGEN AND A GAS INPUT OF 2008 CF/hr

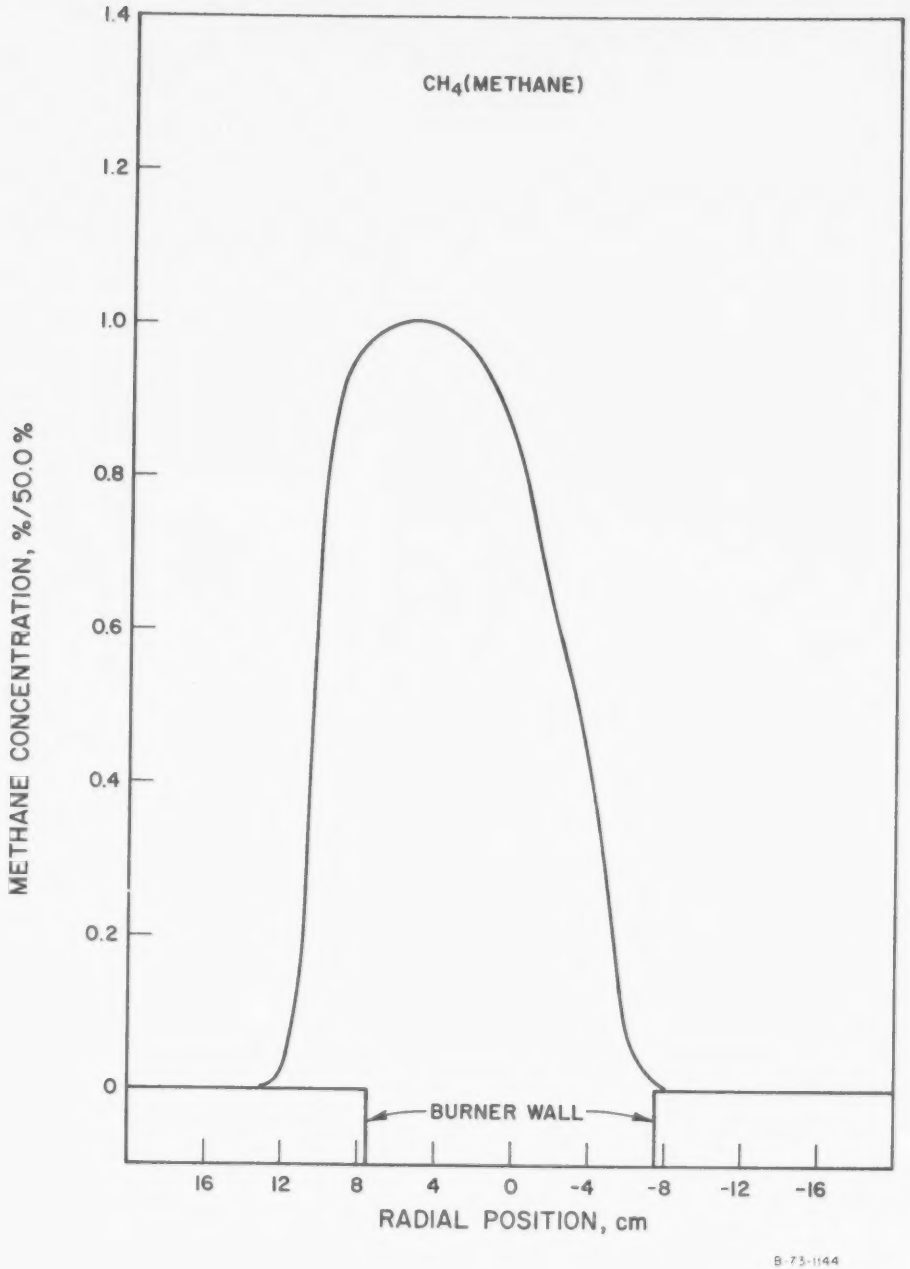


Figure I-38. RADIAL $CH_4$ CONCENTRATION PROFILE FOR THE MOVABLE-BLOCK BURNER AT AN AXIAL PROBE POSITION OF 12.7 cm AND SET FOR INTERMEDIATE SWIRL INTENSITY, GAS NOZZLE IN THROAT POSITION, 3.6% EXCESS OXYGEN, AND GAS INPUT OF 2008 CF/hr

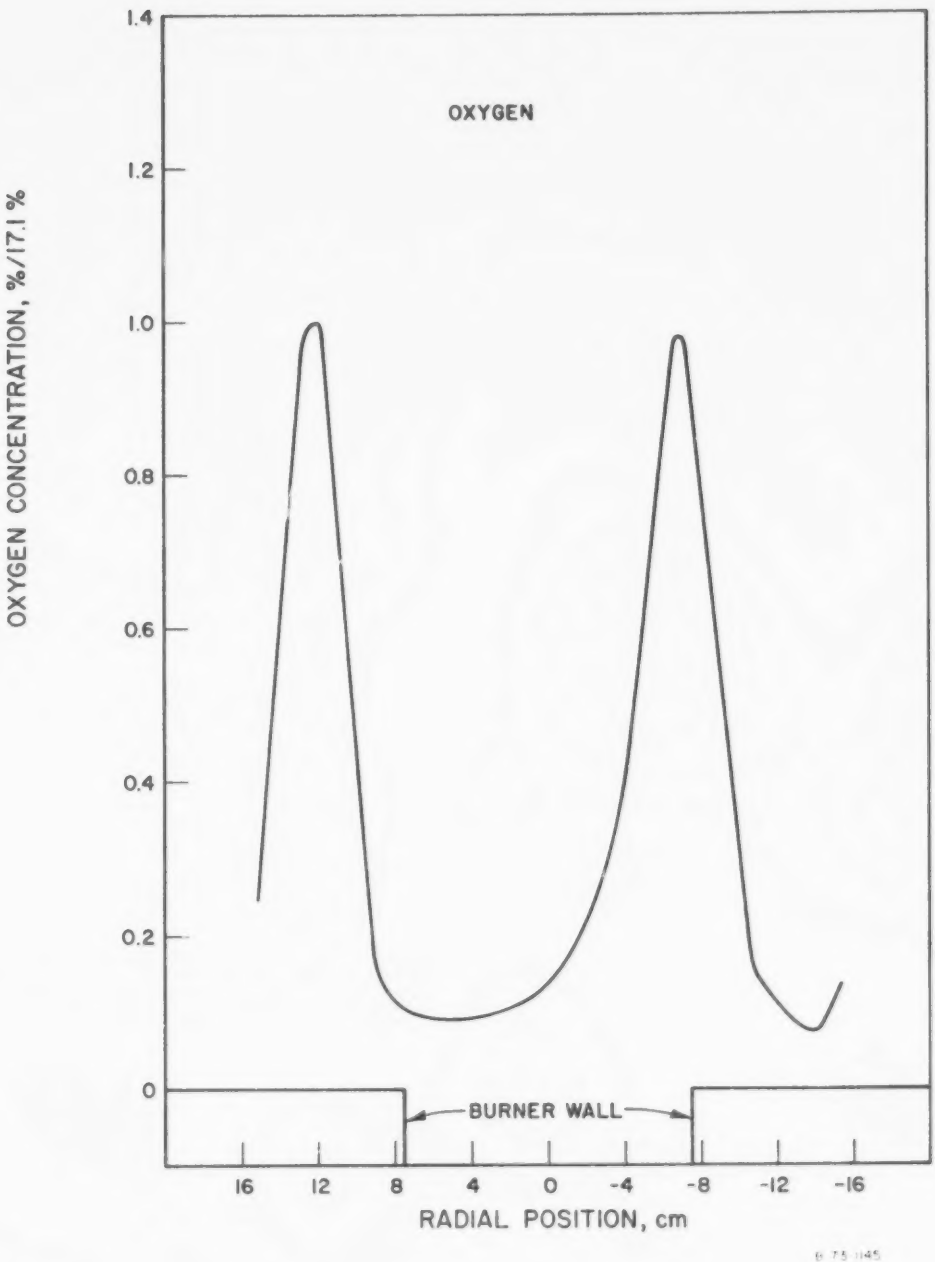


Figure I-39. RADIAL $O_2$ CONCENTRATION PROFILE FOR THE MOVABLE-BLOCK BURNER AT AN AXIAL PROBE POSITION OF 12.7 cm AND SET FOR INTERMEDIATE SWIRL INTENSITY, GAS NOZZLE IN THROAT POSITION, 3.6% EXCESS OXYGEN, AND A GAS INPUT OF 2008 CF/hr

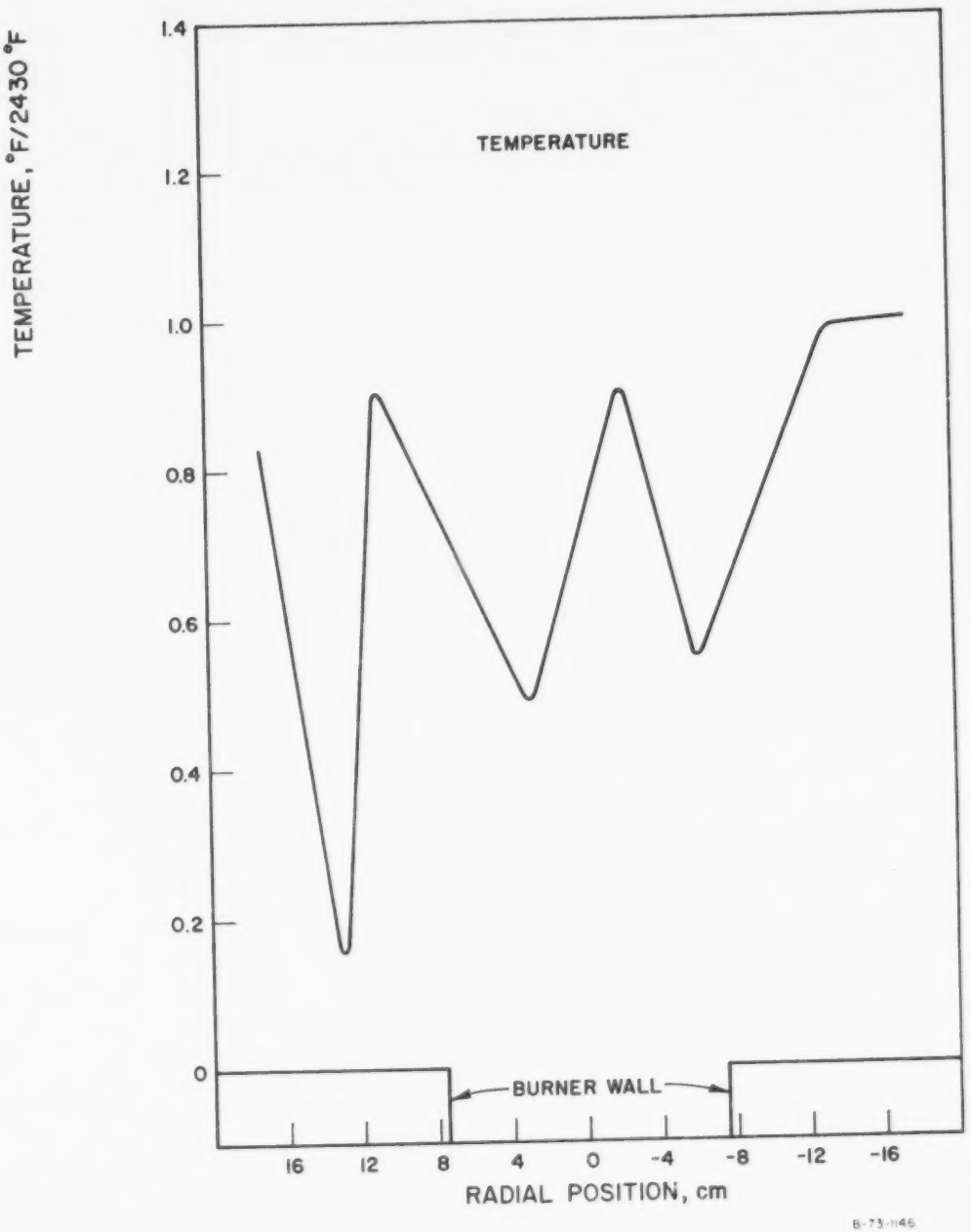


Figure I-40. RADIAL TEMPERATURE PROFILE AT THE 12.7-cm AXIAL POSITION (Movable-Block Swirl Burner – Intermediate Intensity; Gas Input, 2008 CF/hr; Excess Oxygen, 3.6%; Nozzle in Throat Position)

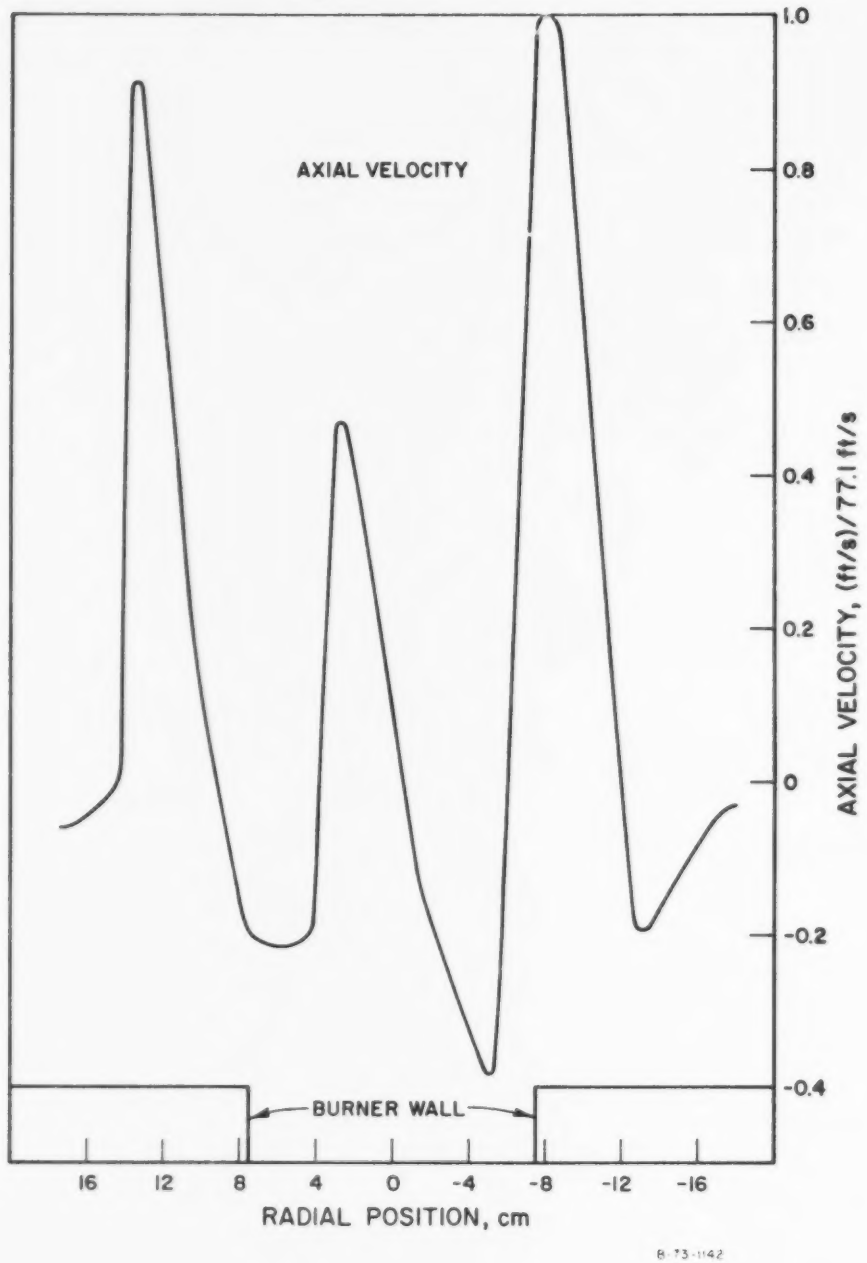


Figure I-41. RADIAL PROFILE OF AXIAL VELOCITY AT THE 12.7-cm AXIAL POSITION (Movable-Block Swirl Burner – Intermediate Intensity; Gas Input, 2008 CF/hr; Excess Oxygen, 3.6%; Nozzle in Throat Position)

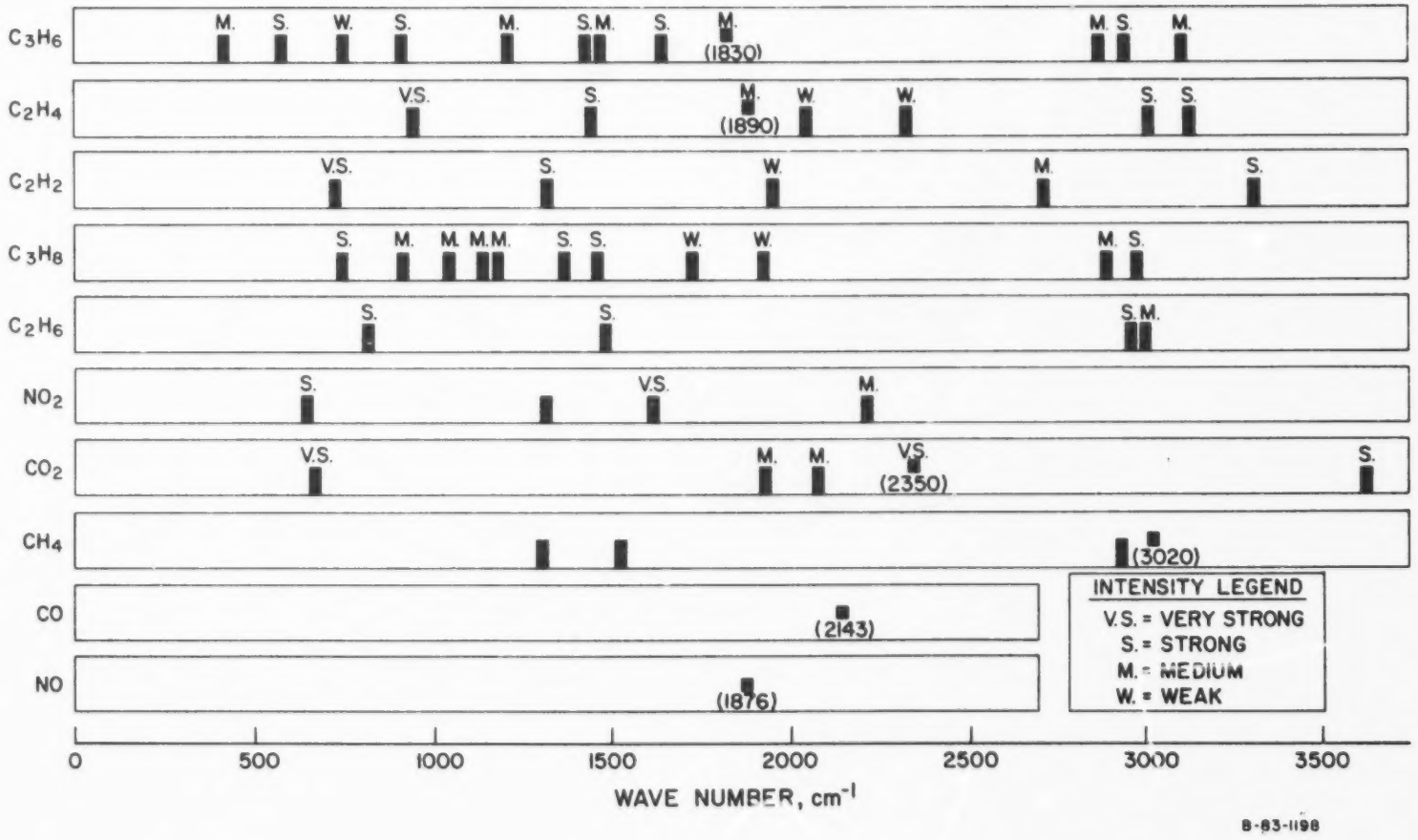


Figure I-42. INFRARED SPECTRA BAND LOCATIONS

removed by the gas-drying system, the tests were performed again introducing the gas samples into the drying system before they were analyzed. The test results were identical to those of the previous investigation. A graphical representation of these experimental relationships between the ethylene or propylene concentration and the equivalent NO concentrations indicated by the NDIR analyzer are shown in Figure I-43. Other optical interferences measured were propane with NO and ethylene and propylene with CO. These interferences were 25 times smaller than the ones reported above and have been disregarded in this report.

To correct the radial position versus NO concentration profiles for these optical interferences, we assumed that the ethylene and propylene concentrations measured at the burner center line decreased radially proportional to the $CH_4$ concentration changes.

The NO concentration radial profile for the movable-block swirl burner can also be corrected for optical interferences. This profile was shown in Figure I-22. The corrected data are represented on the NO transparency (Figure I-37) dashed line. Beyond the region from −6 to 11 cm (where the dashed and solid lines join), there is no correction. As for the "short" flame baffle burner, the profile resembles an upside down script "m" in shape. This profile does not have as much structure as the "short" flame baffle burners profile because the flame has not had as long to develop. The distance between the sampling point and the point of gas injection is only 30 cm for the movable-block burner while it was 53 cm for the "short" flame baffle burner. The temperature profile illustrated in Figure I-24 and the temperature curve in Figure I-40 (transparency) also reflects an upside down script "m" shape, very similar to the temperature profile of the short-flame baffle burner.

Table I-6 gives the mass spectrometer's analysis of a gas sample from the boiler burner taken in the furnace at a 12.7-cm axial position. There were no measurable amounts of either ethylene or propylene. Thus, the NO profile measured for the boiler burner needs no corrections because of optical interferences. Like the boiler burner, all burners which had a Type II flame would burn approximately 95% of the combustibles before the gas entered the furnace. Since there were only trace amounts of methane measured in the furnace, we can conclude that no optical interferences caused by ethylene and propylene occur in a Type II flame.

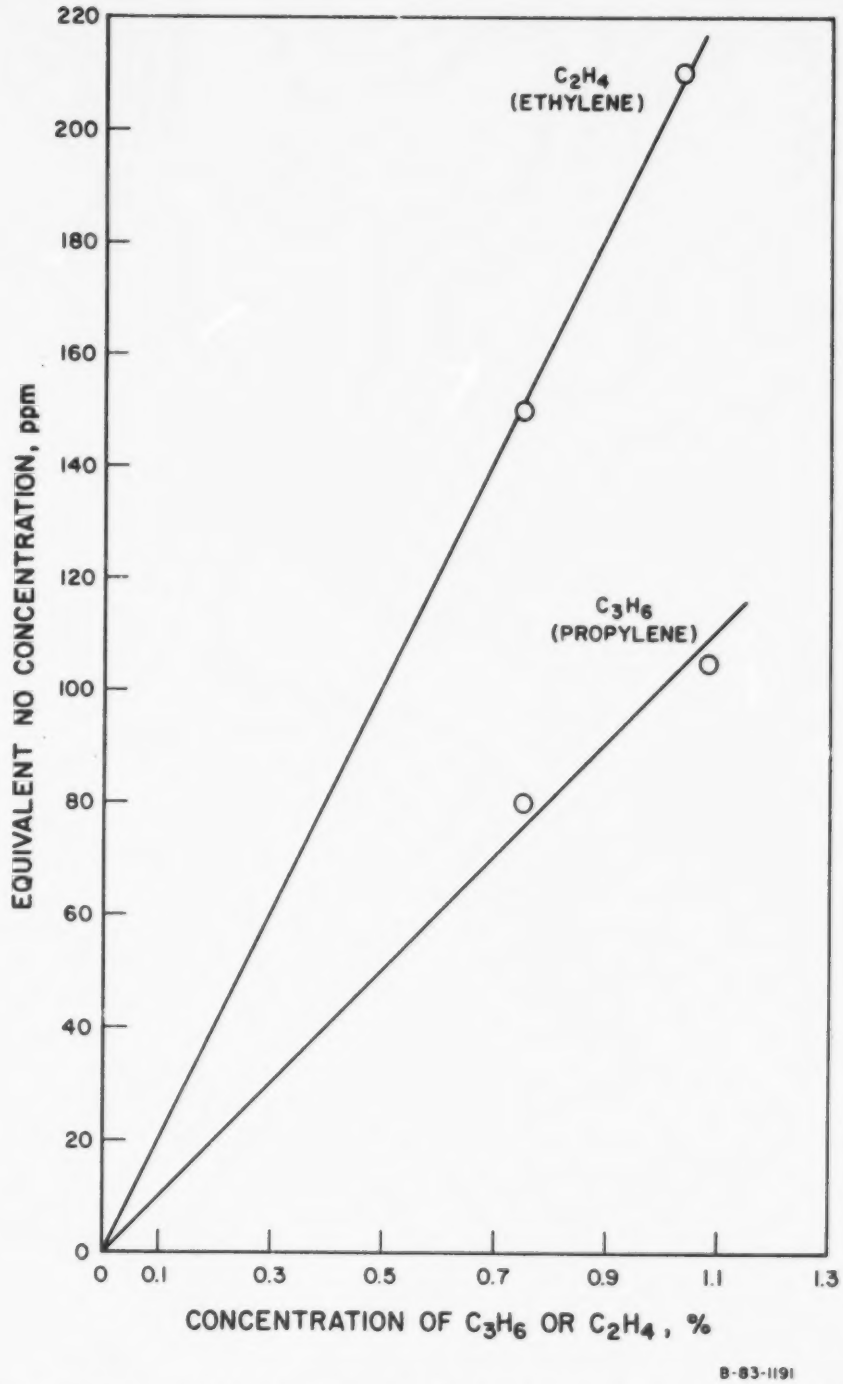


Figure I-43. NO CONCENTRATION CORRECTION FACTORS FOR GAS SAMPLES CONTAINING $C_2H_4$ AND/OR $C_3H_6$

As discussed earlier, there are two types of mean flow patterns: Type I (Figure I-1) is a toroidal recirculation cell, and Type II is a steady pear-shaped recirculating cell. Two burners displayed flow patterns that could not be described by either the Type I or the Type II flow patterns. Tables I-7 and I-8 present direction flow measurements taken for the movable block burner with intermediate swirl intensity, a 2008 CF/hr gas input, and 20% excess air. The probe used in these measurements is described in Volume II of this report. The sign of the time-averaged $\Delta P$ (pressure differential) determines the directional flow of the gases. In Tables I-7 and I-8, a plus sign correlates with forward flow (flow away from the burner) and a negative sign indicates a recirculating flow (flow toward the burner). From Table I-7, we then can deduce that at a 12.7-cm axial position the flow pattern resembles that of a Type I flame. This can be visualized by turning to the axial velocity transparency (Figure I-41) present in this report. However, the data from Table I-8 indicate that the flow pattern at a 30.5-cm axial position resembles that of a Type II flame. Velocity data for the short-flame baffle burner shows a similar type of flow mixture between Type I and Type II patterns.

Figures I-44 and I-45 present two possible flow patterns which can explain these data. Figure I-44 illustrates an unsteady pear-shaped recirculating cell. In this case the recirculating region would oscillate back and forth across the center line. However, because of the frequency resolution of the measuring systems (10 cycles/s) as compared with the frequency of recirculating cells (~4 cycles/s) we should have been able to detect these oscillations. Nonetheless, we detected no oscillations.

Figure I-45 illustrates a kidney-shaped recirculating cell. From the figure, we can see that a radial traverse near the downstream edge of the recirculating cell would indicate a Type I flow pattern while a traverse near the upstream edge of the cell would indicate a Type II flow pattern. Although we plotted the x and y velocity components for the 12.7-cm and 30.6-cm axial positions, a comparison with the stream lines shown in Figure I-45, proved to be inconclusive since we do not know what our position is relative to the recirculating cell. Thus to verify a kidney-shaped recirculating cell would require at least one more directional flow profile.

Table I-7. TIME-AVERAGED DIRECTIONAL FLOW DATA OBTAINED AT THE 12.7-cm AXIAL POSITION (Movable Block Swirl Burner – Intermediate Swirl Intensity). GAS INPUT, 2008 CF/hr; 3.6% EXCESS OXYGEN; NOZZLE IN THROAT POSITION.

| RP,* cm | Time Averaged ΔP | RP,* cm | Time-Averaged ΔP | RP,* cm | Time Averaged ΔP |
|---|---|---|---|---|---|
| 20 | −1.31 | 6 | −7.59 | −3 | −26.37 |
| 17 | −1.11 | 5 | −7.5 | −4 | −20.93 |
| 15 | 0.00 | 4 | −6.3 | −5 | −7.39 |
| 14 | +6.87 | 3 | +0.06 | −6 | −29.87 |
| 11 | +202.0 | 2 | +7.22 | −7 | +148.3 |
| 10 | +204.8 | 1 | +12.37 | −8 | +282.7 |
| 9 | +40.6 | 0 | +12.76 | −9 | +213.0 |
| 8 | −0.1 | −1 | −4.51 | −10 | +91.56 |
| 7 | −5.76 | −2 | −19.31 | −13 | −2.28 |

*Radial Position

Table I-8. TIME-AVERAGED DIRECTIONAL FLOW DATA AT THE 30.5-cm AXIAL POSITION AND OBTAINED USING A HUBBARD PROBE (Movable Block Swirl Baffle – Intermediate Swirl Intensity). GAS INPUT, 2008 CF/hr; EXCESS OXYGEN, 3.6%; NOZZLE IN THROAT POSITION

| RP,* cm | Time-Averaged ΔP | RP,* cm | Time-Averaged ΔP | RP,* cm | Time-Averaged ΔP |
|---|---|---|---|---|---|
| −13 | +55.86 | −1 | −2.09 | 11 | +17.21 |
| −10 | +59.82 | 2 | −3.38 | 14 | +42.63 |
| −7 | +31.52 | 5 | −1.48 | 17 | +33.37 |
| −4 | +4.77 | 6 | −0.88 | 20 | +8.59 |
| −3 | +1.58 | 7 | −0.08 | 23 | +1.08 |
| −2 | −0.94 | 8 | +1.86 | 26 | −0.53 |
| | | | | 29 | −0.77 |

*Radial Position

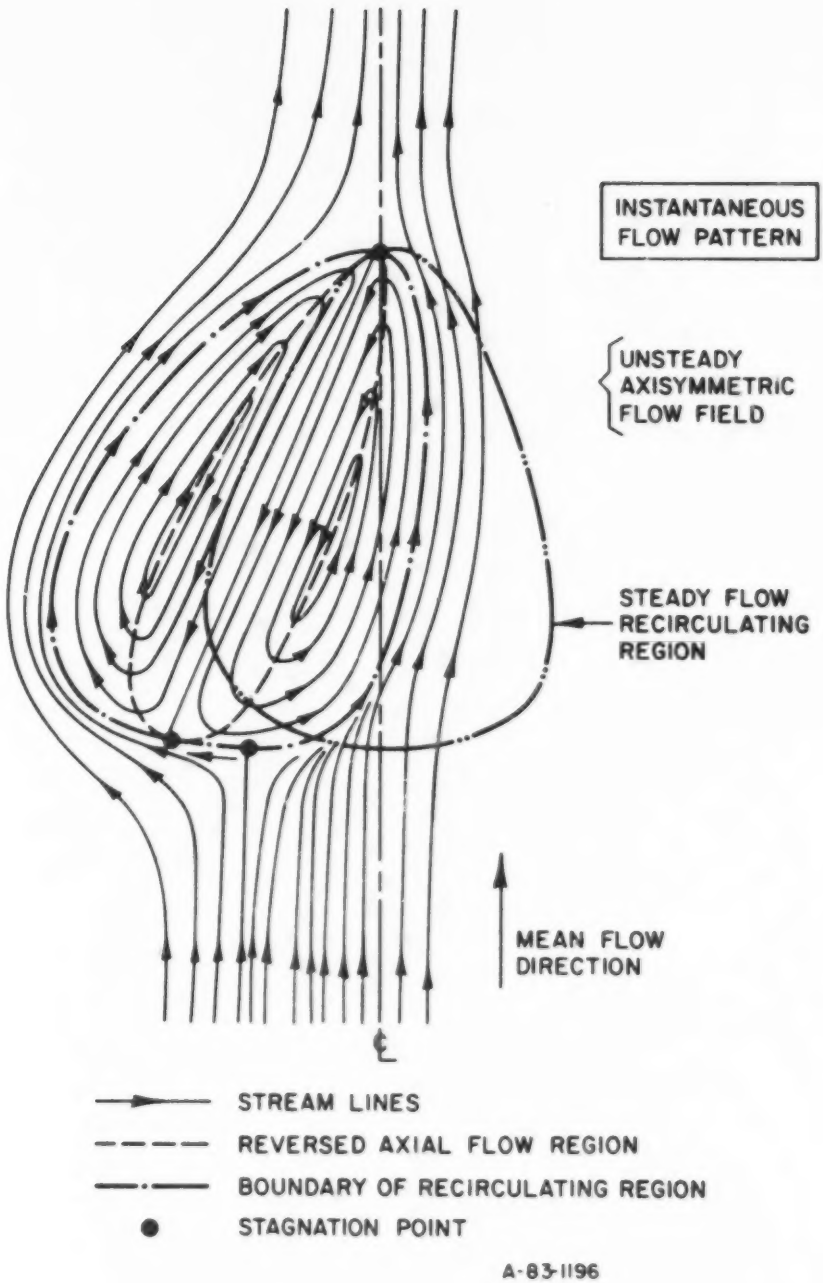


Figure I-44. UNSTEADY PEAR-SHAPED RECIRCULATING CELL

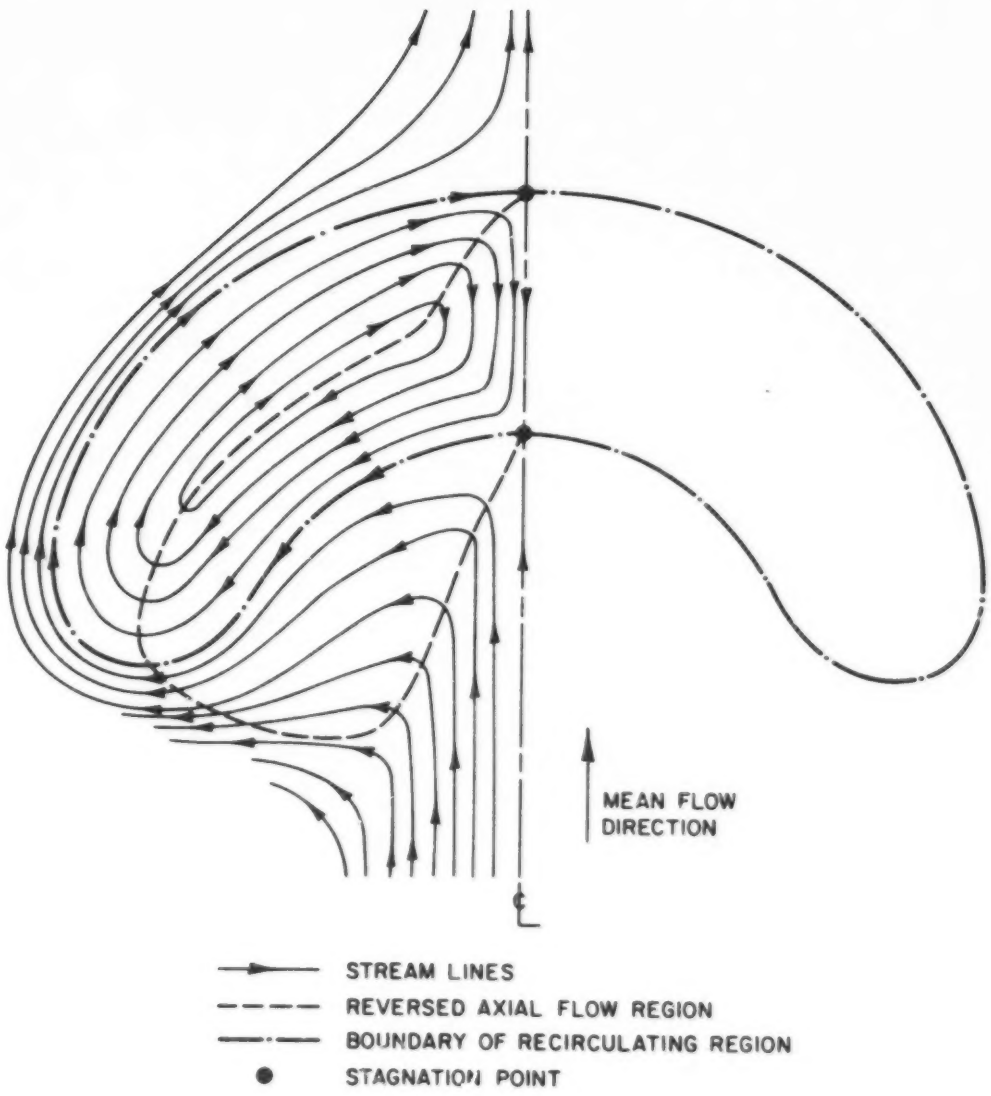


Figure I-45. KIDNEY-SHAPED RECIRCULATING CELL

We can conclude from a survey of the input-output data that the flue concentrations of NO for Type II flow patterns are approximately 3-1/2 times larger than those for Type I flow. A similar difference in the magnitude of NO concentrations can be observed by comparing NO radial profiles. In addition to the flow pattern, a major difference between Type I and Type II flames is the region of combustion. A Type I flame will typically consist of 50% unburned combustibles when it leaves the burner block and enters the furnace while gases of a Type II flame will have less than 10% combustibles. Since 50% of the combustion of a Type I flame occurs in the furnace, a lower flame temperature will result because of the rate of heat release and the diffusion and entrainment of recirculating combustion products. These recirculating combustion products will absorb thermal energy, making less energy available for the kinetics of NO formation.

ACKNOWLEDGMENT

The Environmental Protection Agency gratefully acknowledges the assistance of J. D. Nesbitt, senior adviser, Institute of Gas Technology, for his aid on this project.